Zeitschrift: IABSE reports = Rapports AIPC = IVBH Berichte
Band: 999 (1997)

Rubrik: Codes and standards

Various Tests for Defining the Behaviour of Composite Slabs

Arto TENHOVUORI
M.Sc. Civil Eng.
Helsinki Univ. of Tech.
Espoo, Finland

Arto Tenhovuori, born 1960, received his M.Sc. in 1991. From 1987 to 1993 he worked for a bridge consulting company in Oulu on practical bridge design and joined HUT in 1993. His research into compositestructures has concerned the behaviour of composite slabs.

Matti V. LESKELÄ
Ph.D. Civil Eng.
Univ. of Oulu
Oulu, Finland

Matti Leskelä, born 1945, received his Ph.D. in 1986 and has been carrying out research into composite structures from the early 1980's. His latest work has concerned problems of partial interaction and various shear connections in composite structures such as slim floors, composite slabs and concrete filled steel tubes.

Summary

There are several possibilities for experimentally defining the strength of the shear connection in composite slabs, in which a full plastic bending resistance cannot be reached. Harmonisation of the methods has not been done so far, and the paper discusses the characteristics of various tests such as the slab test to Eurocode 4, its modifications and some small scale tests. The applicability of the partial shear connection method to all slabs, independent of the ductility requirements, is also discussed.

1. Introduction

In EC4 (ENV 1994-1-1 [1]), two methods are given for defining the resistance of composite slabs in the case of shear connection failures: the m-k method and the method based on partial shear connection theory. It is allowed to apply the former method to all slabs, independent of the ductility characteristics of the shear connection, while the applicability of the latter is restricted to slabs having only ductile shear connections. In both methods the behaviour assumed for the design is generalized from six flexural tests, which should represent the essential characteristics of the structural system. The question may then be asked, are the tests required capable of this. It has been shown in various studies that the methods of EC4 for composite slabs should be improved, and there are some rules contradictory with real behaviour.

Some profiles do not meet the ductility definition to EC4, but numerical analyses by the finite element method would show that the behaviour of the slabs with these sheetings is nevertheless ductile enough that it would be appropriate to interprete it consevatively enough according to the partial shear connection theory. The bond strength for the theory, $\tau_{u.R}$, is determined from the results of slab tests with two concentrated loads, and is assumed to be constant, but a considerable variation will be observed when shear spans and slab depths are varied. It is justified to assume that the basic property of the shear connection, the longitudinal shear resistance of the connection per unit length, is constant, but it is the interpretation of the test results in $\tau_{u.R}$ that makes the variation. It is also

possible to apply small scale tests, such as the Australian slip block test [4] and various pull-out tests, but it is not clear if they offer a better solution or not. The problem in real slabs is that different parts in their shear connection do not reach their ultimate resistance at the same instant which contradicts the idealized theories.

2. Forces at connection interface

Both vertical and longitudinal forces are introduced to the connection interface by vertical loads on a slab, but the longitudinal shear forces are mainly considered in the design, as the resistance to these forces controls the bending resistance of the member. Reasonable models are available for the longitudinal forces, but it is quite complicated to evolve the forces that cause vertical separation effects between the sheeting and the concrete accurately. However, their importance in the bonding behaviour has clearly been shown in tests, since the persistency of the interlocking systems depends on their resistance to vertical separation: in flexural tests for common embossments it was observed that the resistance to longitudinal shear in a re-entrant rib-profile was greatly enhanced when its resistance to vertical separation was improved by adding 'elbows' to the corners of the re-entrant ribs. It should also be noted that in all bond tests which are not based on flexure, the separation effects do not appear on the same level as in the bending tests, and in the shear block test [4] the vertical separation is deliberately prevented.

3. Numerical simulation of real slab behaviour

The method based on layered beam elements (LBE) [3] has been used succesfully for simulating various slab tests. It is possible to control both local and global properties of the shear connection so as to include all the essential parameters which affect the behaviour and results in the analyses. Shear connection is modelled as non-linear spring elements for which the load-slip characteristics were initially selected on the basis of tests made on Finnish profiles [2]. Characteristic for them is that they represent good resistance for both vertical separation and longitudinal shear. In order to make parametric studies, reference values for the nominal longitudinal shear strength, $\tau_{u.R}$ (EC4 definition), are related to slabs with total depth h equal to 120 mm and shear spans L_s equal to 350 mm (Fig. 1a). Notation $\tau(h, L_s)$ is used to identify various combinations of slab depth and shear spans, and these are considered with reference to strength $\tau(h, L_s) = \tau(120, 350)$ for which values 0.95, 0.9, 0.59, 0.52 and 0.45 MPa were given.

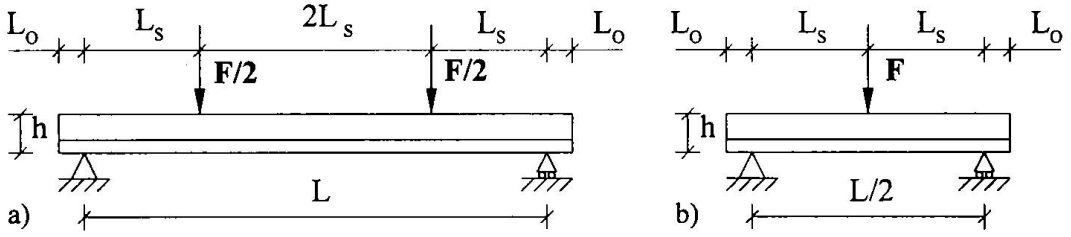

Fig. 1 Load configurations for slab tests: a) two loads according EC4 and b) single central load

3.1 Variability of $\tau_{u.R}$ in slabs with ductile shear connections

Slabs meeting the ductility requirement of EC4 were analyzed using the LBE method, and calculation results interpreted into τ-values are shown in Fig. 2 for various slab depths and shear spans. Uniform loading and loadings according to Fig. 1 above were applied, but for the uniform loading the shear span of L/3 was assumed, as this is in better agreement with the reality than L/4 [2]. According to the results, rate $\Delta M_{test}/\Delta L_s$ shows only minimal variation and is nearly constant. Extrapolation in Fig. 2 is based on this fact.

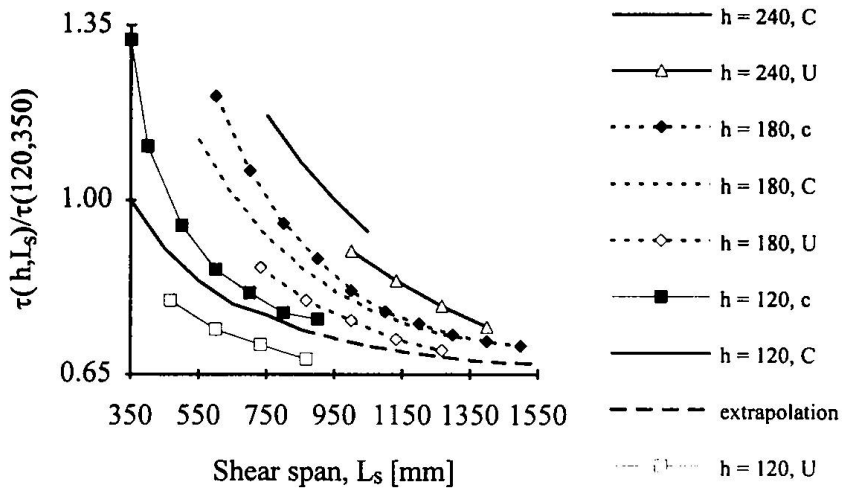

Fig. 2 Bond strength variation for strength level τ(120, 350) = 0.45 MPa in slabs with two concentrated loads according to EC4 (id. = C), a uniformly distributed load (id. = U) and a single concentrated load (id. = c) for different depths h and shear spans L_s of the slab.

3.2 Effect of non-ductility

Non-ductile and ductile behaviour of uniformly loaded slabs are introduced in Fig. 7.12 of ENV 1994-1-1 and the effect of non-ductility was studied by assuming for the connection a load-slip relationship in which the loads drops to 0 or 50 % of the maximum immediately after the peak is passed, and then the load remains constant. Although the cases considered should be classified as brittle, the results were interpreted into $\tau_{u,R}$-values represented as curves with the indentifier 'b' in Fig. 3. The difference in the load drop does not affect the ultimate load of the slabs, as the maximum shear forces are obtained simultaneously on the length of the shear spans. It should also be noted that the difference between ductile (d-curves) and brittle cases (b-curves) in Fig. 3 is only slight, and the trend in the curves is similar to that in Fig. 2.

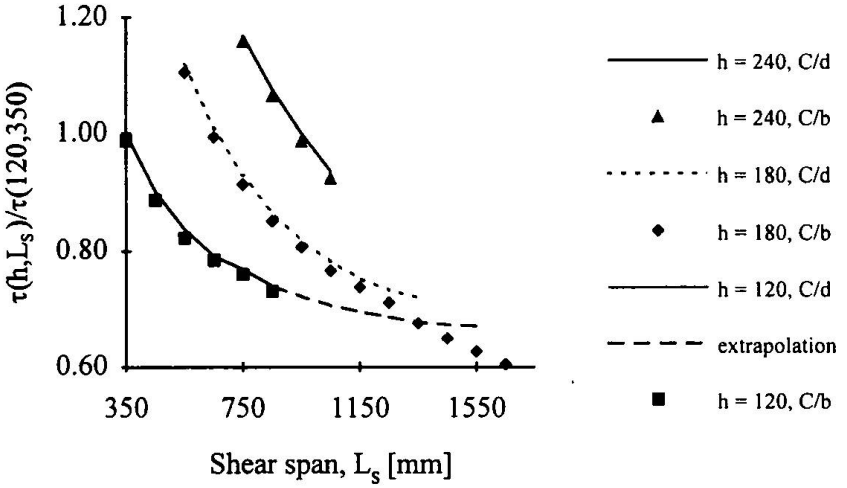

Fig. 3 Bond strength variation for strength level τ(120, 350) = 0.45 MPa for slabs with ductile (id. = d) and non-ductile (id. = b) shear connections and loaded according to EC4. Depth h and shear spans L_s in the slab are varied.

3.3 Effect of additional reinforcement

Additional reinforcements A_s are used in composite slabs for improving their fire resistance and the reinforcement is normally omitted in the normal temperature design, although a method is given in Annex E of ENV 1994-1-1 for the allowance of the bar reinforcement. A constant axis distance of 40 mm was assumed in LBE calculation and the resistances obtained, M_{test}, are compared with the resistance M_{Rd} given in E.5(1) of ENV 1994-1-1, calculated according to variable strength $\tau(h, L_s)$ in which A_s is omitted, i.e. the minimum of the bond strength was not applied, as the real effect of the reinforcement was studied here. In all strength levels considered, similar results were obtained and the curves for $\tau(120, 350)$ = 0.45 MPa are represented in Fig. 4.

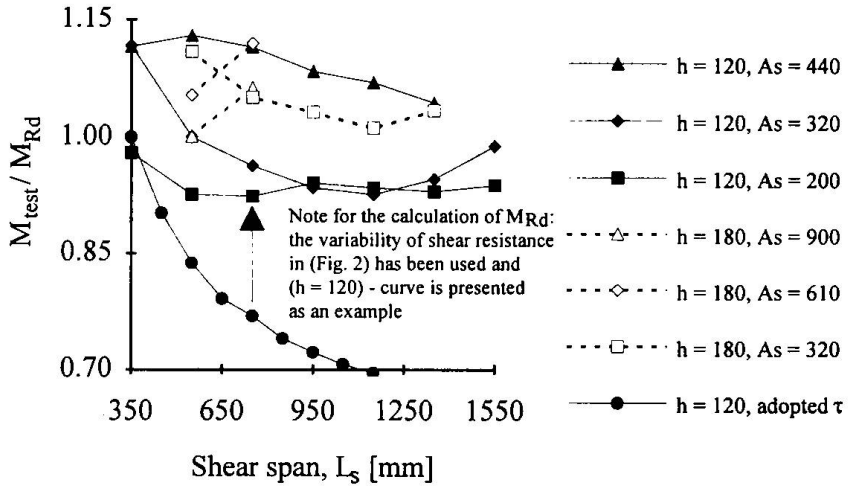

Fig. 4 Variation of bending resistance for slabs having additional reinforcement A_s when depth h and shear spans L_s are varied in slabs with $\tau(120, 350)$ = 0.45 MPa, loaded according to EC4

3.4 Calculation results interpreted by the m-k method

The numerical analyses discussed above were also interpreted into coordinates for the m-k method, and the results for the strength level of the previous figure are shown in Fig. 5. A good correlation into linear regression lines is seen, when constant slab depths are considered, and all the lines cross the vertical axis practically at the same point (k), but there is a large scatter in the inclination (m), showing primarily the effect of the slab depth. The scatter is intensified with smaller strengths of the connection. In order to avoid the scatter in m, a change in the horizontal axis should be made, and it proved best to multiply the original axis by the effective depth of the slab, d_p, i.e. $A_p d_p/(bL_s)$ will be the new axis. Thereby a practically constant m is obtained in Fig. 6 for the data of Fig. 5 and there is now scatter in the values of k, the importance of which in the resistance evaluation is smaller, however.

3.5 Effect of friction at supports and number of failure mechanisms

The Australian shear block test [4] considers the friction in the shear interface, and due allowance is made for it in the design of slabs. In the LBE analyses friction at supports may be considered locally or globally as distributed to the length of the effective connection. The latter option is the one applied in the analyses above, and accordingly the strengths employed for the shorter shear spans are slightly higher than in reality. When the resistance of the slab decreases, the effect of friction will also become smaller, whereas in thicker slabs with short shear spans the share of friction in the resistance will be higher. In fact, the reason why the lines in Fig. 5 do not cross the vertical axis exactly at the same

point can be explained by means of friction: for shallow slabs the true scatter would be larger than that presented here and for thick and short slabs it would be smaller in the case where the friction is taken into account in the most appropriate manner, i.e. as a summary the effect of friction will not invalidate the principles of the behaviour presented above.

In laboratory tests it is frequently observed that clearly higher ultimate loads are obtained in such slabs where both ends are failing simultaneously due to excessive slipping, as compared to the cases of single end failure which represent the determining values. This can be explained by means of energy considerations. A symmetrical failure presupposes that the bond properties are very uniformly distributed along the shear spans which is typical of slabs with high bond strength. Then it is also expected that the overall scatter would be smaller.

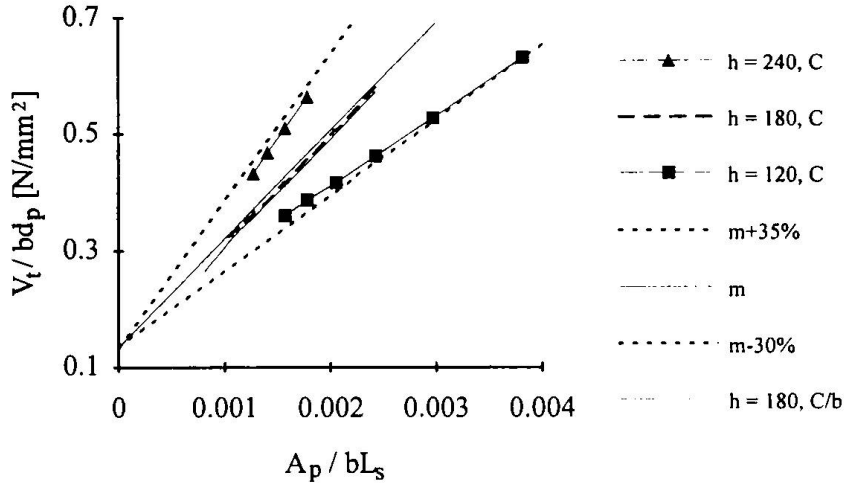

Fig. 5 Various analyses of slabs loaded according to EC4 and interpreted according to the m-k method, assuming that τ(120, 350) = 0.45 MPa, and h and L_s are varied. Coordinates are as given in EC4 [1].

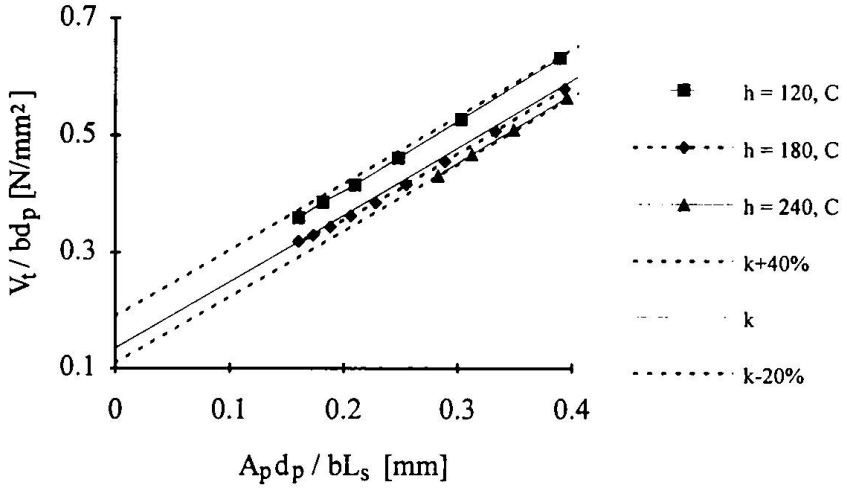

Fig. 6 Various analyses of slabs loaded according to EC4 and interpreted according to the modified m-k method, assuming that τ(120, 350) = 0.45 MPa, and h and L_s are varied. Coordinates given in EC4 are modified in the horizontal axis.

4. Conclusions

The bond strength will decrease with increasing shear span and it will increase with increasing slab depth, independent of load distribution, and the minimum value for this strength is obtained from slabs with a minimum depth (see Figs. 2 and 5). The smaller the average bond strength, the higher is the scatter in the results. The best strength, relatively, is obtained by employing a single concentrated load on the slab, and the strength will become gradually smaller when the load configuration is changed towards more uniform distribution (Fig. 2). For long shear spans the results approach an asymptote represented by the minimum value obtained from the double load test in EC4. Thus it would be cost-efficient to employ a single load configuration when long shear spans are required.

Ductile and non-ductile shear connections that have similar resistance per unit length behave basically in the same manner when shear spans not longer than one metre are concerned and the test results are interpreted according to the partial shear connection method, but for longer shear spans with non-ductile connections smaller strengths than for ductile connections of similar resistance will be obtained (Fig. 3). Therefore there should be no reasons for not allowing the use of this method for a wide range of so-called non-ductile connections, as it is always possible to apply a greater reduction when evaluating the characteristic value of $\tau_{u,R}$. In the m-k method the non-ductility has practically no influence on the regression line, due to the coordinate axes employed, and this is also seen in Fig. 5 in which one non-ductile set of results (identifier C/b) is presented together with ductile sets.

The principal effect of additional reinforcing bars is to improve the bond strength by reducing the crack widths, and the mode of failure can change to pure bending. All the results in Fig. 4 satisfy the requirement, $M_{test} \geq 0.9M_{Rd}$, and the additional tests required for reinforced slabs in EC4 are thus not necessary.

It was clearly shown that the m-k method is well suited for evaluating the resistance of slabs with respect to connection failures, and a reliable value for parameter k is obtained when constant depth is used for all specimens, varying only the length of the slabs (Fig. 5). For the reliability of the results, the minimum depth employed in practice should be selected for tests. Various depths of the slab represent clearly different values for parameter m, and the results will not be rational when varying depth are used in the regression analysis, i.e. the inclination of such line will be arbitrary. If the horizontal axis is modified so as to include the effect of the slab depth, the inclination of the regression lines will represent the real behaviour as far as constant depth is used in all tests, and it only remains to decide a reliable value for k. It should be noted that when working in the coordinates proposed, the slabs with the maximum depth are the determining ones, which is opposite to the τ_u method. It is finally pointed out that the research reported in this paper also includes principles for interfacing the m-k method and its modifications with the partial shear connection method, and a calculation formula was derived with which any single tested bond strength τ_u can easily be converted into other values of τ_u for other shear spans, while keeping the depth of the slab constant. This makes it possible to re-evaluate old tests for the harmonisation purposes.

References

[1] Eurocode 4 (1992). "Design of Composite Steel and Concrete Structures, Part 1-1: General rules and rules for buildings", ENV 1994-1-1:1992. CEN

[2] Tenhovuori, A., Kärkkäinen, K. and Kanerva, P. "Parameters and Definitions for Classifying the Behaviour of Composite Slabs". Composite Construction III, Proceedings of an Engineering Foundation Conference, Irsee, Germany, 1996.

[3] Leskelä, M.V. (1992) "A Finite Beam Element for Layered Structures and Its Use when Analysing Steel-Concrete Composite Flexural Members". Constructional Steel Design: World Developments, 354-358. Elsevier Applied Science

[4] Patrick, M., (1990) "A New Partial Shear Connection Strength Model for Composite Slabs". Journal of the Australian Institute of Steel Construction, V.24, No3, 2-17

On the Strength Headed Shear Studs in Solid Slabs

Michelle RAMBO-RODDENBERRY
Via Doctoral Fellow
Virginia Polytechnic Inst. and State Univ.
Blacksburg, VA, USA

W. Samuel EASTERLING
Associate Professor of Civil Eng.
Virginia Polytechnic Inst. and State Univ.
Blacksburg, VA, USA

Thomas M. MURRAY
Montague-Betts Professor of Struct. Steel Design
Virginia Polytechnic Insti. and State Univ.
Blacksburg, VA, USA

Summary

A series of 24 solid slab push-out specimens were tested. Twelve of the tests were performed to investigate the effect on the shear stud strength of the flange thickness to which the stud was welded. In six tests, the steel/concrete interface was changed to investigate the influence of friction at the interface. In sic tests the normal load applied to the specimens was varied to establish the influence on the shear stud strength. The test results show that flange thickness does not affect shear stud strength and that significant friction is developed at the interface.

1. Introduction

The results of 24 solid slab, shear stud push-off tests that were recently conducted at Virginia Polytechnic Institute and State University (VPI&SU) are reported in this paper. The purposes of the tests were (1) to further examine the effect of beam flange thickness on shear stud strength and (2) to examine the contribution of friction at the slab/beam interface to stud strength. The test program to date consisted of eight series of tests with three identical tests in each series. Series 1-4 (Tests 1-12) are used to examine the effect of beam flange thickness on shear stud strength, while Series 5-8 (Tests 13-24) are used to evaluate the contribution of friction to the slab/beam interface.

2. Description of Tests

All test specimens were constructed with the same stud diameter, stud length, stud tensile strength, number of stud connectors per slab, and steel reinforcement. Each series consisted of three tests. For series 1-4 (tests 1-12), the flange thickness to which the stud was welded was varied by using different steel sections. For series 5 and 6 (tests 13-18), only the slab/beam interface was varied. For series 7 and 8 (tests 19-24), only the amount of normal load applied to the specimen was changed. The purpose of these tests is described below.

2.1 Flange Thickness Influence

The first parameter evaluated was the influence on shear stud strength of the thickness of the flange to which the stud is welded. The majority of the push-out tests performed at VPI&SU have used WT155x26 sections, with a nominal flange thickness of 13.2 mm. The writers wished to verify that thinner or thicker flanges would cause no change in stud strength. A stud diameter of 19 mm was used for all tests, and the concrete strength was kept the same. A total of 12 push-out specimens were tested. The desired mode of failure was stud shearing; thus, the diameter-to-flange thickness ratio was kept below 2.7, as recommended by Goble (1968).

Goble (1968) first investigated the behavior of thin flange push-out specimens. From 41 specimens with 13 mm, 16 mm or 19 mm shear studs, he determined a relationship, based on the beam flange thickness, that indicates the point at which the failure mode changes from stud shear to flange pull out. Beam flange thicknesses between 3 mm and 11 mm were used. Concrete strengths varied among the tests. Goble concluded that flange pull out occurs when the ratio of stud diameter to flange thickness is above 2.7.

2.2 Slab/Beam Interface Influence

The second parameter investigated was the effect of friction at the slab/beam interface. The writers wanted to determine if the *apparent* stud strength was reduced by reducing the interaction between the concrete and beam flange. The apparent stud strength is that determined from the push-out test, which includes any effect contributing to the load resistance. Six push-out tests were conducted with a piece of flat sheet steel placed at the interface. Three of the specimens had a layer of lithium grease placed between the sheet steel and beam flange. These two series, along with Series 7, which had no sheet steel at the interface, permit an examination of the interface influence.

An upper limit for the shear stud strength of $A_{sc}F_u$ is used in the American Institute of Steel Construction (AISC) specification (*Load* 1993). The limit appears inconsistent given that it represents the tensile strength of the shear stud, when in fact the behavior of the stud is generally described in terms of shear. If the strength was controlled by a shear limit state, using a failure theory such as von Mises', the upper limit would be expected to be $0.6A_{sc}F_u$. However, the argument for the higher limit appears justified when the test data that were used to formulate the AISC specification provisions are considered (Ollgaard, et al 1971).

Lyons, et al (1994) postulated that the inconsistency between the AISC specification equation and described behavior was due to friction at the slab/beam interface. The friction at the interface, which is present in typical solid slab push-out specimens results in an apparent stud strength that is greater than that predicted using a shear limit state in the stud. The presence of steel deck reduces the friction at the interface, thus reduces the apparent strength of the shear studs.

2.3 Normal Load Influence

The third parameter investigated, which is directly related to the friction at the interface, was the influence on stud strength of normal load applied to the test specimen. Previous solid slab specimens tested at VPI&SU did not have normal load applied. Tests performed with formed steel deck, however, did have normal load applied. To further investigate the effect of friction at the slab/beam interface, six identical push-out specimens were tested. A normal load of 10% of the axial load was applied to three of these specimens. The 10% normal load is used in push-out tests to simulate gravity load on a composite beam (Sublett, et al, 1992). No normal load was applied to the other three specimens. If the amount of normal load applied causes a difference in strength, this is evidence that either friction is being developed or that the state of stresses in the stud is being changed.

3. Specimen Construction and Loading Procedure

All push-out specimens were constructed using wooden forms. Specimens were 915 mm by 915 mm, and consisted of a 146 mm thick normal weight concrete slab on a WT section. Tests 1-3 and 13-24 used WT155x26; the studs were welded over the web of the steel section. Tests 4-6 used WT155x26, tests 7-9 used WT155x19.5, and tests 10-12 used WT205x42.5; studs were welded off-center for these tests. The stud size used for all tests was 19 mm x 105 mm. Material tests conducted by the shear stud manufacturer indicated a tensile strength, F_u, of 448 MPa. Two studs were used in each specimen half, spaced at 460 mm along the length of the flange. Steel reinforcement was the same for all tests: two layers of four 10 mm reinforcing bars placed on the bottom of the slab, and two layers placed on the top. When sheet metal was used, holes were precut in the metal so that the studs were welded directly to the steel beam. All specimens were cast horizontally.

Series 1-4 were cast using the same batch of concrete, Series 5 and 6 were cast together, and Series 7 and 8 were cast together. The specimens were covered and moist-cured for seven days, at which time the forms were removed. Concrete test cylinders were cast along with the specimens and cured similarly. The halves were then bolted through the webs to form a push-out specimen.

Axial load was applied and measured with a hydraulic ram and load cell. In some tests, a load was applied normal to the slab surface using a yoke device placed around the specimen. The normal load was applied using a hydraulic ram and measured with a load cell. Axial load was applied in increments of 22 kN until a load of approximately 80% of the expected capacity was reached. After that, displacement control was used. For the tests with normal load, each axial load increment was preceded by a normal load increment of approximately 10% of the axial load.

4. Test Results

Test results, as well as stud strength calculations using the AISC specification (*Load* 1993), are summarized in Table 1. The failure mode was stud shearing for all tests reported. Series 1, where the studs were welded over the web of a WT155x26 (t_f = 13.20 mm), had an average experimental load per stud of 118.9 kN. The studs were not welded over the web in Series 2-4. Series 2, where the studs were welded on a WT155x26 (t_f = 13.20 mm), had an average experimental load per stud of 117.8 kN. Series 3, which used a WT155x19.5 (t_f = 9.10 mm), had an average experimental load per stud of 114.2 kN. Series 4, which used a WT205x42.5 (t_f = 18.20 mm), had an average experimental load per stud of 112.5 kN. As seen from Fig. 1, flange thickness does not significantly affect stud strength. Also, the experimental stud strengths were underestimated by the AISC equation. The average load at stud failure for Series 1-4 was 1.13 times the AISC predicted value.

Series 5-6, which had sheet metal placed between the concrete and steel, show that there is no significant change in stud strength when the steel/sheet metal interface is greased. The average stud strength when the interface was greased was 105.8 kN, and the average stud strength when the interface was not greased was 110.3 kN. It does seem that by eliminating the steel/concrete interface by using sheet metal, the stud strength is significantly reduced. This conclusion can be made by comparing Series 5 and 6 with Series 7. These series have approximately the same concrete properties. The only difference between the tests was the use of sheet metal in Series 5 and 6, and none in Series 7. Series 7 had an average shear stud strength of 130.6 kN, which is 23% greater than series 5 and 18% greater than series 6. This demonstrates that when steel deck is used, even without a profile rolled in the deck as in series 5 and 6, the stud strength is less than for a solid slab.

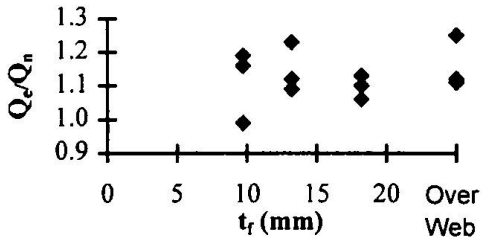

Fig. 1 Effect of flange thickness on stud strength

Series 7 resulted in a higher stud strength than series 8. In series 8, where normal load was not applied, the average stud strength was 114.2 kN. The normal load increases the frictional resistance from the slab and beam.

Series	Test	Stud Loc.	t_f (mm)	Concrete Strength f'_c (MPa)	Concrete Weight w (kN/m^3)	Percent Normal Load	Calculated Load Per Stud Q_n (kN)	Experimental Load Per Stud Q_e (kN)	Ratio Q_e/Q_n	Failure Mode
1	1	C	13.2	23.7	21.8	10	102.4*	114.6	1.12	SS
	2	C	13.2	23.7	21.8	10	102.4*	128.2	1.25	SS
	3	C	13.2	23.7	21.8	10	102.4*	113.7	1.11	SS
2	4	F	13.2	23.7	21.8	10	102.4*	126.4	1.23	SS
	5	F	13.2	23.7	21.8	10	102.4*	112.1	1.09	SS
	6	F	13.2	23.7	21.8	10	102.4*	115.0	1.12	SS
3	7	F	9.7	23.7	21.8	10	102.4*	101.8	0.99	SS
	8	F	9.7	23.7	21.8	10	102.4*	118.6	1.16	SS
	9	F	9.7	23.7	21.8	10	102.4*	122.4	1.19	SS
4	10	F	18.2	23.7	21.8	10	102.4*	115.8	1.13	SS
	11	F	18.2	23.7	21.8	10	102.4*	113.0	1.10	SS
	12	F	18.2	23.7	21.8	10	102.4*	108.5	1.06	SS
5#	13	C	13.2	32.2	22.7	10	127.5**	106.9	0.84	SS
	14	C	13.2	32.2	22.7	10	127.5**	109.4	0.86	SS
	15	C	13.2	32.2	22.7	10	127.5**	101.2	0.79	SS
6#	16	C	13.2	32.2	22.7	10	127.5**	109.4	0.86	SS
	17	C	13.2	32.2	22.7	10	127.5**	106.9	0.84	SS
	18	C	13.2	32.2	22.7	10	127.5**	114.6	0.90	SS
7	19	C	13.2	33.6	22.7	10	127.5**	132.2	1.04	SS
	20	C	13.2	33.6	22.7	10	127.5**	127.4	1.00	SS
	21	C	13.2	33.6	22.7	10	127.5**	132.2	1.04	SS
8	22	C	13.2	33.6	22.7	0	127.5**	104.9	0.82	SS
	23	C	13.2	33.6	22.7	0	127.5**	118.6	0.93	SS
	24	C	13.2	33.6	22.7	0	127.5**	119.2	0.93	SS

SS = Stud Shearing

C = studs welded centrally on beam

F = studs welded off-center on beam

Series 5 & 6 used flat sheet metal between the steel beam and concrete
Series 5 was greased between the sheet metal and beam

$* = 0.5 A_{sc} \sqrt{f'_c E_c}$ $\quad ** = A_{sc} F_u$

Table 1 Test results summary

5. Conclusions

Based on the limited number of tests conducted to date, the following conclusions are made:

1. Experimental stud strengths were between 79% and 125% of the AISC predicted value.
2. Flange thickness, for the stud diameter-to-flange thickness ratios tested in this paper, has little or no influence on the strength of a stud.
3. Adding flat sheet metal between the steel and concrete in a solid slab specimen significantly reduces the stud strength obtained in a push-out test.
4. Applying a normal load to a test specimen measurably increases the stud strength.
5. Based on the tests reported, the lack of friction between the concrete and steel significantly reduces the apparent shear stud strength.

6. Notation

A_{sc} = cross sectional area of a shear stud
f'_c = concrete compressive strength
F_u = tensile strength of shear stud
Q_e = experimental strength of shear stud
Q_n = nominal strength of a shear stud (note that calculations in the paper made with measured material properties)
t_f = flange thickness of steel section

7. References

Goble, G. G. (1968). "Shear Strength of Thin Flange Composite Specimens." *Engineering Journal*, AISC, 5(2), 62-65.

Load and Resistance Factor Design (LRFD) Specification for Structural Steel Buildings (1993). American Institute of Steel Construction, Inc. (AISC), Chicago, IL.

Lyons, J. C., Easterling, W. S. and Murray, T. M. (1994). "Strength of Welded Shear Studs." Report No. CE/VPI-ST 94/07. Virginia Polytechnic Institute and State University., Blacksburg, VA.

Ollgaard, J. G., Slutter, R. G. and Fisher, J. W. (1971). "Shear Strength of Stud Connectors in Lightweight and Normal Weight Concrete." *Engineering Journal*, AISC, 8(2), 55-64.

Sublett, C. N., Easterling, W. S. and Murray, T. M. (1992). "Strength of Welded Headed Studs in Ribbed Metal Deck on Composite Joists." Report No. CE/VPI-ST 92-03. Virginia Polytechnic Institute and State University, Blacksburg, VA.

Shear Resistance of Stud Connectors with Profiled Sheeting

Roger P. JOHNSON
Professor of Civil Eng.
University of Warwick
Coventry, Great Britain

Hui YUAN
Research Student
University of Warwick
Coventry, Great Britain

Summary

The static resistance to shear of stud connectors welded through profiled steel sheeting is a complex function of over 20 parameters. Study of the results of 269 push tests shows that none of three recent sets of design rules is valid over the full range of parameters. All can give errors around ± 30 %. Results are given of 34 new push tests, in accordance with Eurocode 4. Models are developed for 7 modes of failure. They lead to rules that predict all relevant test results (172) with a mean error of 2% and a coefficient of variation of 9.5%.

1. Introduction

Profiled steel sheeting is widely used as permanent formwork for composite floor slabs in buildings. Stud shear connectors for composite beams are placed in troughs in the sheeting, the span of which is normally either transverse to or parallel with the span of the beams. Predictions of the static shear resistance per stud, P_r, are based on resistances P_e found in push tests, and are often presented, as in draft Eurocode 4:Part 1.1 [1], in the form $P_r = kP_{rs}$, with $k \leq 1$, where P_{rs} is the resistance of a stud in a solid slab of the same concrete, and k is a reduction factor.

For many re-entrant profiles (e.g., Holorib, Bondek II), studs can be so located that $k \approx 1$. The many trapezoidal profiles in use give lighter composite slabs; but the studs may be less efficient ($k < 1$), especially where there are two per trough with one placed on the 'unfavourable' side (denoted U here) of a central rib (e.g., as in Fig. 1). In such situations, all recent design methods known to the authors have errors of prediction exceeding ± 30%. They do not identify which of the many failure modes is critical, and do not include all relevant parameters.

This paper is a summary of an extensive search for better design methods [2], more fully reported elsewhere [3]. It was found that the resistance P_r can be influenced by over 20 independent parameters. They are now listed, with relevant notation:

- the eight dimensions shown in Fig. 1, and the strength f_{yp} of the sheeting;
- the cylinder strength f_c, density ρ, and stiffness E_{cm} of the concrete;
- the ultimate strength f_u of the studs, and their number N_r per concrete rib;
- the spacings and positions of the studs relative to the sheeting: single studs in Unfavourable, Central, or Favourable positions in a trough of the sheeting, and pairs of studs loaded in Series, in Parallel, or in a Diagonal arrangement. (The upper case letters U, C, etc., are used below to refer to these layouts);

- the use of through-deck or through-hole welding;
- the use of non-standard push tests, especially with studs at only one level in each slab, or with the slabs 'on end' when cast;
- the size, spacing, and level in the slab of reinforcement, if any.

Most publications of push-test results fail to give data on all these parameters, and few describe modes of failure. This led to the exclusion of many reported results from this work, the stages of which are now listed.

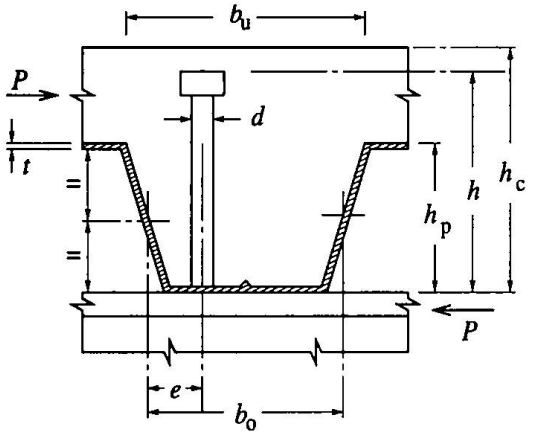

Fig. 1 Shear connector in a composite slab

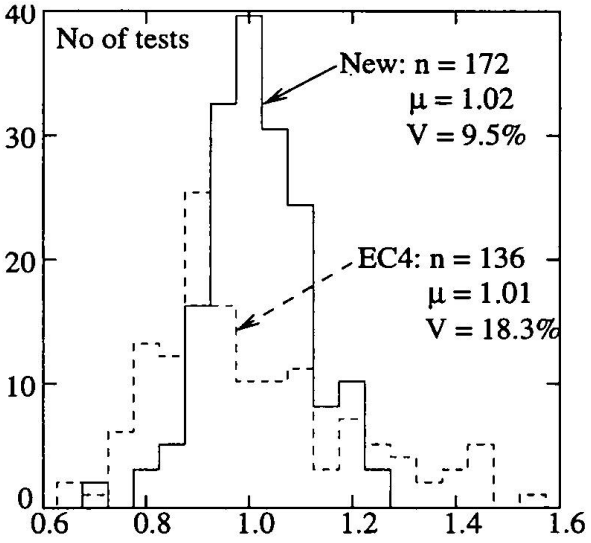

Fig. 2 Histograms of P_e/P_r for 172 push tests

2. Method, and principal conclusions

(1) All available push-test results (269) were studied, and 66 that lacked data were rejected. This left only 20 with parallel sheeting, so that statistical work was done for transverse sheeting only. The 183 other results were placed in 8 groups, according to the method of welding, the number N_t of troughs per slab, and N_r. It was found using the statistical t and F tests and the design rules of Eurocode 4 that, with 95% probability, these data were samples from seven different populations. The 14 through-hole results were about 20% weaker than the others, so they were excluded from further study. This left five groups, with $8 \le n \le 66$, where n is the number of samples (tests) per group.

Table 1. Ranges of ratios P_e/P_r, with P_r given by three methods, after mean-value correction, for five layouts of studs

Range of:	1, central	1, unf.	1, fav.	2, parallel	2, series
b_o/h_p	0.7 - 2.6	2.4 - 3.2	2.0 - 3.2	1.3 -3.1	2.0 - 3.2
δ_{EC}	0.7 - 1.3*	0.7 - 1.1	0.9 - 1.4	0.6 -1.4*	0.7 - 1.4
δ_L	0.7–1.3*	0.8–1.4	0.8–1.2	0.6–1.2*	0.7–1.2
δ_H	0.8–1.3			0.7–1.3	

*excluding one very high result

(2) Three design methods were studied, denoted by subscripts EC, for Eurocode 4; L, for a proposal by Lawson [4], and H, for work by Hanswille [5]. For each test and design method, the ratio b_i (= P_e/P_r) was found, and the mean value μ_b calculated for each group and design method. Values δ, given by $\delta = P_e/\mu_b P_r$, were then found. Their ranges are given in Table 1 for each group and design method. It is evident that, even with mean-value correction, each method has errors of at least $\pm$ 30%, and for more than one group. The most important independent variable is probably the breadth/depth ratio of each trough, b_o/h_p, so the ranges of values present in these data are also given.

(3) The widest gaps in the data were narrowed by doing 34 new push tests, as specified in Eurocode 4. There were 17 matched pairs, which included 6 different profiles, with ratios b_o/h_p (Fig. 1) ranging from 1.75 to 3.2; three sheet thicknesses; three concrete densities; single studs in U, C, and F positions; and pairs of studs in S, P, and D arrangements. In most specimens the slab reinforcement, a light mesh, was at or above the heads of the studs. Its influence, if any, was neglected in subsequent work. The load-slip curves are on record [2]. The slip capacities, defined as the slip at which the load first fell to 80% of its peak value, ranged from 2 mm to 16 mm, based on the lower of the results from a pair of tests. The 17 pairs of failure loads per stud differed, on average, by only 3%, which is exceptionally low for push tests.

The observed failure modes are denoted:

- CPT, concrete pull-out; SS, shank shear; RP, rib punching; and combinations of these, for transverse sheeting;
- CPP, concrete pull-out; and SP, splitting, for parallel sheeting.

(4) Theoretical models for the prediction of the failure mode and the resistance P_r were developed for each of the five modes for transverse sheeting and two for parallel sheeting. The introduction of new parameters, such as the thickness of the sheeting, reduced the number of existing tests with sufficient known data from 203 to 138, plus the 34 new ones. These results were used to determine certain coefficients in the expressions for P_r so that, as expected, the mean of the 172 values was, at 1.02, close to 1.0. The significant result is evident in the histogram of P_e/P_r for the new methods (Fig. 2), for which the coefficent of variation is only 9.5%, less than half that previously achieved. For example, the histogram for tests with transverse sheeting given by the methods of Eurocode 4, Fig. 2, has V = 18.3%, and that for parallel sheeting (36 tests) has μ = 1.66, V = 35%.The failure mode was predicted correctly for all the tests except 9, where CP failure was predicted, and SS failure occurred, at a higher load.

(5) The new expressions for prediction, outlined in the next Section, are rather complex; but their use does not involve trial and error. If they are applied to studs and sheeting of given properties, with a given layout of studs, the properties of the concrete are the only independent variables.

Advantage was taken [2] of the implicit inter-relationships that exist between the combinations of the parameters that occur in practice, to develop simpler but empirical resistance functions for studs in transverse sheeting, as described elsewhere [3]. They give a histogram of 136 values of P_e/P_r with μ = 1.03, V = 10.5%. Thus, the simplified rules are almost as good as the more complex ones; but they are not based on mechanical models, and should not be used outside their defined scope.

(6) Both the general and the simplified methods give predictions for the mean value of the resistance P_r. The characteristic value P_{rk} and the partial safety factor γ_M ($= P_{rk}/P_{rd}$, where P_{rd} is the design value) should be based on statistical analyses. The number of sets of data, n, exceed 20 for only one group of the data, tests on transverse sheeting with one stud per trough and two troughs per slab, for which $n = 51$. Analysis of this group led to: $P_d = 0.75\, k\, P_{rs}/\gamma_M$, with $\gamma_M = 1.25$, the value given in Eurocode 4. There are many reasons [3] why the authors consider that the coefficient 0.75 is too low. It should probably be increased to between 0.9 and 0.95; but that still leaves a step, when $k \approx 1$, of between 5% and 10% between the new method and that of Eurocode 4, because in that code, the 0.75 factor is 1.0.

Test data are not yet sufficient to show clearly how best to bridge this gap, so the main basis for the safety level of design rules will continue to be experience rather than theory. However, it is clear that the new models and rules provide more accurate predictions of both modes and mean resistances than do any others known to the authors.

The areas most in need of new test data are parallel sheeting; lightweight concrete; transverse sheeting with two studs per trough; minimum spacings of pairs of studs; and the influence of transverse reinforcement, especially on slip capacity.

3. Theoretical models, for both normal-density and lightweight concrete

3.1. Shank shearing, SS, for transverse sheeting

This is the expected mode of failure of a stud in a well-reinforced solid slab. The resistance was assumed to be as given in Eurocode 4 [1], and to be the upper limit for failures by other modes:

$$P_{rs} = 0.37\, A_s\, (f_c\, E_{cm})^{0.5} \leq 0.2\, \pi\, d^2 f_u. \qquad (1)$$

The limit set by the strength f_u of the stud material did not govern, in the present work. For the other modes of failure, $P_r = k_t\, P_{rs}$, with $k_t \leq 1$.

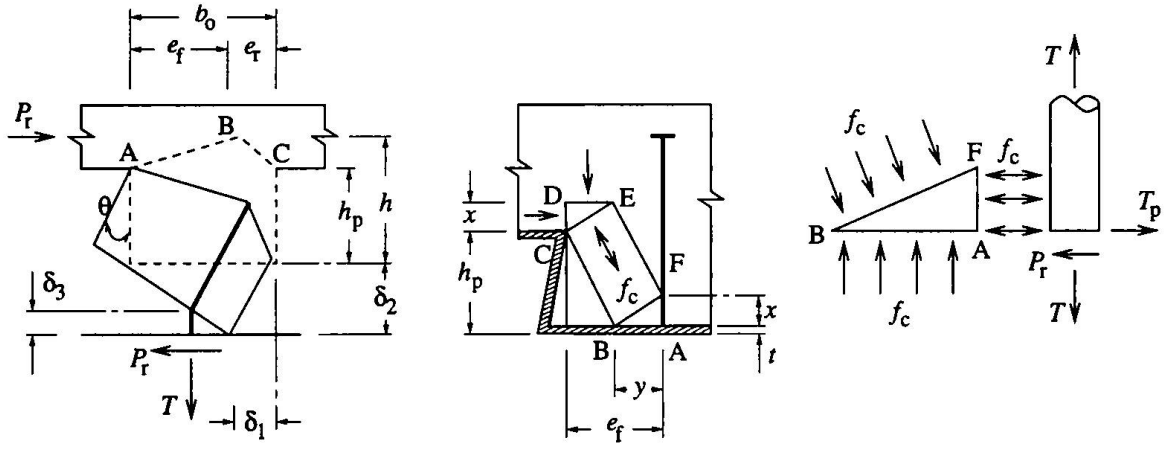

(a) (b) (c)

Fig. 3 Models for failure modes CP and RP, for transverse sheeting

3.2. Concrete pull-out, CP, for transverse sheeting

This mode is shown in Fig. 3(a). The slab is assumed to be free to separate from the steel beam. Torsional shear failure occurs at each end of a prism of concrete that includes the stud. Using a von Mises-type yield criterion for the stud and a rigid-plastic model for the concrete leads to

$$k = [\eta + \lambda(1 + \lambda^2 - \eta^2)^{0.5}] / (1 + \lambda^2) \quad (2)$$

where $$\eta = 0.45 f_c^{0.5} h^2 (b_o - h/4) / (h_p N_r P_{rs}), \text{ with } h \le 2h_p \quad (3)$$

$$\lambda = e_r T_y / (h_p P_{rs}) \quad (4)$$

and $$T_y = 0.2 \pi d^2 f_u \quad (5)$$

with notation as in Figs 1 and 3. The model is applicable where the number of studs per rib, N_r, is 1 or 2, and they are in locations C or F. If equation (3) gives $\eta > 1$, $\eta = 1$ is assumed. Equation (2) then gives $k = 1$, and shank failure is predicted.

3.3. Rib punching, RP, for transverse sheeting

This mode, shown in Figs 3(b) and (c), governs for studs in 'unfavourable' positions (i.e., $e_f < b_o/2$). At failure, a prism of concrete, of cross-section ABCDEF and length b_c, is assumed to be at uniform stress f_c. The force $b_c f_c y$ that it applies across surface AB is assumed to be equal to the tension T in the stud. The shear force P_r applied to the stud is resisted by the reaction $b_c f_c x$ from the concrete and force T_p arising from yielding of the sheeting in tension over a length b_p, normal to the cross-section shown. Analysis of this model and use of the test results leads [3] to equation (2) for k, with

$$\eta = 1.8 (e_f + h - h_p) t f_{yp} / P_{rs} \quad (6)$$

$$\lambda = e_f T_y / (2 h_p P_{rs}). \quad (7)$$

Where a pair of studs is placed with one near each side of a rib, one fails in mode RP and the other in mode CP.

3.4. Splitting failure and concrete pull-out failure, for parallel sheeting

The derivation of the following expressions is given elsewhere [3]. The model for splitting failure is based on extensive work by Oehlers [6]. Splitting of a long prism, with cross-section EHLI in Fig. 4, is caused by a patch load P_r on area FGKJ. The result is

$$P_r = 2.4 \pi f_c^{0.5} [e^3 h_{es} / (2e - d)^2 + h_c^3 d / (2h_c - h_{es})^2] \quad (8)$$

with h_{es} given by $$(h_{es} - h_p) / (h - h_p) = 0.56 [2.4 - 2e / h_p], \le 0.5. \quad (9)$$

Concrete pull-out failure occurs when the mean tensile stress on a pyramidal surface of area A_c, enclosing the stud(s), reaches the tesile strength of concrete. The total tensile force is deduced from the splitting theory, and expressions for area A_c are easily obtained for any layout of studs within the trough. The final result for a single stud is

$$P_r = 0.6 f_c^{0.5} [4 \pi e^3 h_{ep} / (2e - d)^2 + A_c] \quad (10)$$

where $$h_{ep} = 2 h_c [1 - (\pi d h_c / A_c)^{0.5}]. \quad (11)$$

Height h_{ep} is equivalent to h_{es} in Fig. 4, and this mode governs where $h_{ep} < h_{es}$.

4. Conclusions

(1) These conclusions relate to the static shear resistance P_r of stud shear connectors with $f_u \geq 400$ N/mm^2 welded through steel sheeting of trapezoidal profile with $0.8 \leq b_o/h_p \leq 3.2$ (see Fig. 1), in concrete with $20 \leq f_c \leq 35$ N/mm^2, and projecting at least 35 mm above the sheeting. Restrictions on stud spacing, data on slip capacity, and more detailed results are given elsewhere [2,3]. The many conclusions given in Section 2 above are not repeated here.

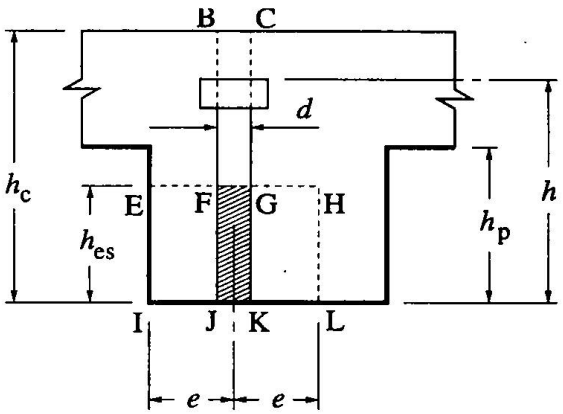

Fig. 4 Patch load for splitting failure

(2) Regions with sparse test data were explored in 34 new push tests, in accordance with Eurocode 4 [1]. The resistances P_e found in these tests and in 169 others show that predictions by all of three recent design methods include errors of at least ± 30% (Table 1).

(3) Seven failure modes have been identified, and methods developed for predicting the critical mode and the failure load, P_r. A histogram of 172 ratios P_e/P_r that includes all the failure modes (Fig. 2) shows a mean ratio $\mu = 1.02$, with coefficient of variation $V = 9.5\%$, much better than for the predictions of Eurocode 4 for transverse sheeting only. Its predictions for parallel sheeting give ratios that range from 0.76 to 2.9.

(4) Simpler design equations, not based on mechanical models, have been developed [3]. Their predictions for the same 136 tests with transverse sheeting give $\mu = 1.03$, $V = 10.5\%$.

(5) The results are for mean resistances, from push specimens with at least four studs. Test data from beams are so sparse and insensitive to the resistance of small groups of studs that the codification of design values must continue to be based as much on experience as on testing. The present work enables current rules to be improved.

5. References

1. DD ENV 1994-1-1, Eurocode 4, 'Design of composite steel and concrete structures, Part 1.1: General rules and rules for buildings', British Standards Institution, London 1994.
2. Yuan, H. 'The resistances of stud shear connectors with profiled sheeting'. PhD thesis, University of Warwick, January 1997.
3. Johnson, R.P. and Yuan, H. 'Resistance of stud shear connectors in troughs of profiled sheeting'. Submitted for publication, 1997.
4. Lawson, R.M. 'Shear connection in composite beams', *Steel Constr. Today*, 171-176, July 1992.
5. Hanswille, G. 'Shear resistance of headed studs with profiled steel sheeting'. Tech. Paper H7, Bergische Universitat, Gesamthochschule Wuppertal, Dec. 1993.
6. Oehlers, D.J. and Bradford, M.A. 'Composite steel and concrete structural members: fundamental behaviour'. Pergamon, Oxford, U.K., 1995.

Application of Eurocode 4 Design Provisions to High Strength Composite Columns

Andrew KILPATRICK
Senior Lecturer in Civil Eng.
University of Southern Queensland
Toowoomba, Qld, Australia

Andrew Kilpatrick received his BEng. degree from the CIAE in 1974, MEngSc degree from the University of Queensland in 1985 and PhD degree from Curtin Univ.

Tracey TAYLOR
Design Engineer
Farr, Evrat and Associates
Toowoomba, Qld, Australia

Tracey Taylor received her BEng. degree from the University of Southern Queensland in 1997 after 3 years working with various consulting civil engineering companies.

Summary

Concrete-filled steel tubular (CFST) columns offer significant structural and economic benefits in a wide variety of applications in the construction industry. This paper examines the applicability of the EC4 simplified method of design to CFST columns which use high strength concrete. Measured column strengths reported in the literature are compared with those predicted by EC4 and, on the basis of the 146 columns analysed, conclusions are drawn on the suitability of the present EC4 provisions to high strength CFST columns.

1. Introduction

Concrete-filled steel tubular (CFST) columns have increased in popularity as the significant number of advantages they offer in both design and construction have come to be appreciated. In recent years high strength concrete, in excess of 60 MPa, has become commercially available for use in construction. If the economic benefits of this material are to be fully realised, then the provisions of design codes must be extended to include high strength concrete. Eurocode 4 (EC4) is, arguably, the pre-eminent code in the world for the design of CFST columns and the aim of this paper is to examine the applicability of the EC4 simplified method of design to CFST columns which use high strength concrete.

2. EC4 Strength Criteria for CFST Columns

In the usual design situation for a member subjected to combined compression and uniaxial bending, the design action effects at the ends of the column N_{Sd} and M_{Sd} are generally known from a structural analysis, and it is then required to find a cross-section size which satisfies the strength criteria given in Eq. (1) and (2).

$$N_{Sd} \leq \chi N_{pl.Rd} \tag{1}$$

$$M_{max.Sd} \leq 0.9 \mu M_{pl.Rd} \tag{2}$$

The maximum moment that the column must support - $M_{max.Sd}$ - may be either at the end of the column or somewhere along its length, and provisions are available (EC4 1992; Bergmann et al 1995) to estimate this moment.

In experiments, however, columns of known length and section size are tested to determine the maximum force $N_{max.meas}$ that they can support. This force is applied either concentrically or eccentrically to the longitudinal axis of the column. Consequently, the analysis of this data requires an approach opposite to that of the usual design situation. Two variations of this approach are possible. Firstly, use the maximum measured force $N_{max.meas}$ to generate a predicted value of the maximum moment along the column and compare this with the measured value. Secondly, use some analytical method to calculate the maximum moment along the column (as a function of the applied force) and predict the corresponding maximum force that the column can sustain. The first method requires a knowledge of the position of the critical section where the bending moment will be largest and measurements of deflection taken at this point. This is possible only in simple cases such as equal eccentricities of force but even so, in many cases, this data is either not measured or reported. This effectively precludes the first method. Because of this, the second method was adopted here, and this has the added benefit of more closely reflecting the process used in design. In the context of the EC4 design procedure and notation, the load N_{Sd} effectively equates to the predicted maximum eccentric force $N_{max.pred}$ under the action of a co-existing moment at the end of the column $M_{Sd} = N_{Sd} \times e$. Because of the complicated inter-relationships between applied force and moment and the interaction curve of the cross-section, the process becomes iterative, eventually converging upon the predicted column strength $N_{max.pred}$.

3. Method of Analysis

In order to allow the analysis to proceed, it is necessary to know the following data:

(i) dimensions of the steel tube, b and h or D, and wall thickness t
(ii) yield stress f_y and modulus of elasticity E_a of the steel tube
(iii) concrete cylinder strength f_{cyl}
(iv) column length L, and
(v) eccentricities of the applied load at the top e_t and bottom e_b of the column

Steps in the analytical procedure are as follows:

1. Check the cross-section for local buckling.
   For a rectangular section: $h/t \leq 52\,\varepsilon$
   For a circular section: $D/t \leq 90\,\varepsilon^2$
   where $\varepsilon = \sqrt{235/f_y}$ with f_y in units of MPa

2. Set the material partial safety factors to unity.
   Hence $f_{yd} = f_y/\gamma_{Ma} = f_y/1.0$
   and $f_{cd} = f_{ck}/\gamma_c = f_{cyl}/1.0$

3. Calculate the Euler buckling load N_{cr} for the column.

$$N_{cr} = \frac{\pi^2 (EI)_e}{L^2} \tag{3}$$

where $(EI)_e = E_a I_a + 0.8 \frac{E_{cm}}{1.35} I_c$

$E_{cm} = 9\,500\,(f_{cyl} + 8)^{1/3}$ MPa, the secant modulus of the concrete from Eurocode 2, for f_{cyl} in MPa

I_a and I_c are the second moments of area of the steel tube and uncracked concrete respectively

and L is the buckling length of the column. In the present study, this was taken to be the column length quoted in the literature.

4. Compute the relative column slenderness $\bar{\lambda}$.

$$\bar{\lambda} = \sqrt{\frac{N_{pl.R}}{N_{cr}}} \tag{4}$$

where $N_{pl.R} = A_a f_{yd} + A_c f_{cd}$

and A_a and A_c are the cross-sectional areas of the steel tube and concrete respectively.

5. Calculate the plastic resistance of the cross-section $N_{pl.Rd}$ to axially applied force.

For a rectangular cross-section:

$$N_{pl.Rd} = A_a f_{yd} + A_c f_{cd} \tag{5}$$

For a circular cross-section in which the effect of confinement may be included:

$$N_{pl.Rd} = A_a f_{yd} \eta_2 + A_c f_{cd} \left(1 + \eta_1 \frac{t}{D} \frac{f_y}{f_{cyl}} \right) \tag{6}$$

where, if both the relative slenderness $\bar{\lambda} \le 0.5$ and the eccentricity ratio $e / D \le 0.1$,

$$\eta_1 = \eta_{10} \left(1 - \frac{10e}{D} \right)$$

$$\eta_2 = \eta_{20} + (1 - \eta_{20}) \frac{10e}{D}$$

$$\eta_{10} = 4.9 - 18.5\bar{\lambda} + 17\bar{\lambda}^2 \quad \text{but} \not< 0.0$$

$$\eta_{20} = 0.25(3 + 2\bar{\lambda}) \quad \text{but} \not> 1.0$$

otherwise, $\eta_1 = 0$ and $\eta_2 = 1$

6. Check whether the column is defined to be a composite column.

The ratio δ must lie within the range $0.2 \le \delta \le 0.9$

where $\delta = \frac{A_a f_{yd}}{N_{pl.Rd}}$

7. Calculate the reduction factor under axial load using the buckling curve "a".

$$\chi = \frac{1}{\Phi + \sqrt{\Phi^2 - \bar{\lambda}^2}} \tag{7}$$

where $\Phi = 0.5 \left[1 + 0.21(\bar{\lambda} - 0.2) + \bar{\lambda}^2 \right]$

8. Select a trial value of $N_{max.pred}$ ($\equiv N_{Sd}$) taken to be the predicted strength of the column.

9. Calculate the associated (predicted) maximum bending moment along the column $M_{max.Sd}$ using the proposal of Bergmann et al (1995).

$$\text{If } N_{max.pred}/N_{cr} \leq \left(\frac{\cos^{-1} r}{\pi}\right)^2 \quad \text{then} \quad M_{max.Sd} = M_{R.Sd} \tag{8}$$

$$\text{otherwise} \quad M_{max.Sd} = \frac{M_{R.Sd}}{\sin \varepsilon}\sqrt{r^2 - 2r\cos\varepsilon + 1} \tag{9}$$

where $M_{R.Sd}$ is the larger of the moments at the end of the column and is equal to $N_{max.pred}$ × (the larger of the end eccentricities e_t or e_b)

$$\varepsilon = \pi\sqrt{\frac{N_{max.pred}}{N_{cr}}}$$

r = ratio of smaller to larger moments (eccentricities) at the end of the column, positive for single curvature bending ($-1 \leq r \leq +1$)

10. Evaluate the resistance of the section to pure bending, $M_{pl.Rd}$

The resistance of the section under pure bending $M_{pl.Rd}$ was evaluated using a computer programme (Goode 1996) designed to determine the force-moment interaction diagram for the cross-section. (Comparisons between the output from this programme and the interaction curves provided by Bergmann et al (1995) were almost identical.) This analysis assumes a full plastic distribution of stresses in the concrete (f_{cd} in compression, zero in tension) and the steel (f_{yd} in compression and tension). (Alternatively, eq.(27) and (28) given by Bergmann et al (1995) may be used.)

11. Calculate the moment ratio μ required to satisfy the moment criterion.

$$M_{max.Sd} = 0.9\,\mu\,M_{pl.Rd} \tag{10}$$

For eccentrically loaded columns where the bending moment at the end is due solely to the action of the eccentricity of the force, the value of μ may exceed 1.0.

12. Determine the imperfection moment ratio μ_k.

Using the computer programme (Goode 1996), the value of μ_k corresponding to χ on the cross-section interaction curve was determined - Figure 1. This was done by selecting different neutral axis depths until the load ratio was equal to χ; the resulting moment ratio was the required value of μ_k.

13. Evaluate the moment ratio μ_d and force ratio χ_d.

After setting $\chi_n = \chi(1-r)/4$ such that $\chi_d \geq \chi_n \geq 0$, values of μ_d and χ_d were evaluated by an iterative process using the cross-section interaction curve until the following was satisfied:

$$\mu = \mu_d - \mu_k \frac{\chi_d - \chi_n}{\chi - \chi_n} \tag{11}$$

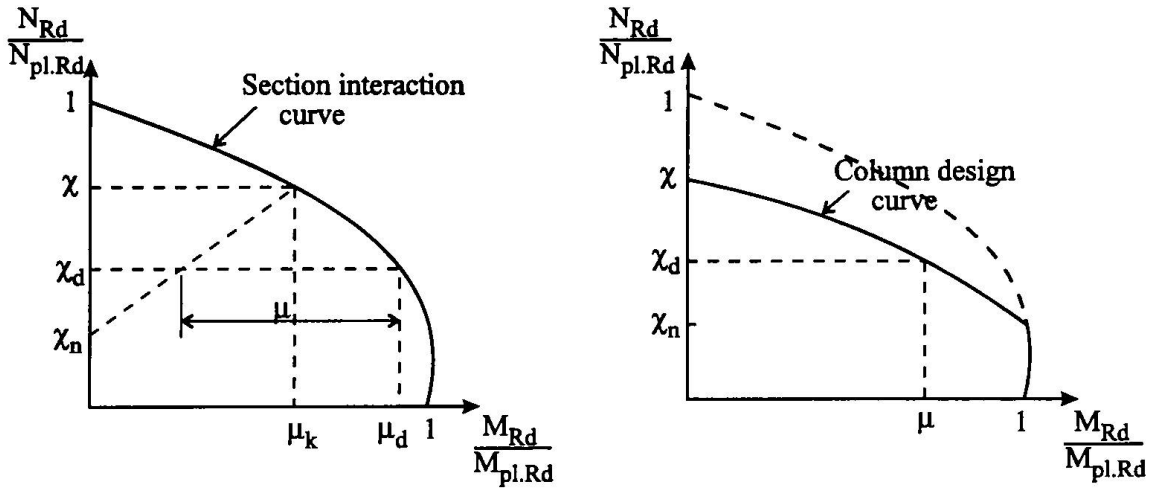

Figure 1 Design for compression and uniaxial bending

14. Compute the new value of predicted column strength $N^*_{max.pred}$.

$$N^*_{max.pred} = \chi_d \times N_{pl.Rd} \quad (12)$$

15. Identify the final predicted column strength $N_{max.pred}$.

Compare the trial value of the force $N_{max.pred}$ initially assumed in step 8 with the value $N^*_{max.pred}$ calculated in step 14. If the two agree to within a prescribed tolerance - a value of 1 kN was selected in the present investigation - the predicted column strength is taken as $N_{max.pred}$. Otherwise select a new trial column strength, by interval halving or some other technique, and return to step 8.

Column strengths predicted by this analysis were then compared with measured data reported in the literature.

4. Analysis of Laboratory Test Data

A total of 146 columns from 6 different investigations were analysed. The concrete cylinder strength ranged from 23 MPa to 103 MPa. Predictions of column strength versus concrete cylinder strength are presented in Fig. 2 which suggests no evidence of any significant effect of the strength of the concrete upon the quality of the column strength prediction. Similarly, no relationship could be detected with the other major parameters of slenderness *L/D*, which varied from 4.0 to 31.6, or eccentricity ratio *r* which varied from +1 to -1 (Kilpatrick and Taylor 1997).

5. Discussion and Conclusions

For the 146 columns analysed, the mean ratio of measured/predicted column strength was 1.10 with a standard deviation of 0.13. EC4 safely predicted the failure load in 73% of the columns analysed. There was no obvious relationship between concrete cylinder strength and the

accuracy of the prediction of column strength. Based on this, it is suggested that EC4 can reliably predict the short-term strength of eccentrically loaded slender CFST columns, including those using concrete strengths in the range of 50 to 100 MPa.

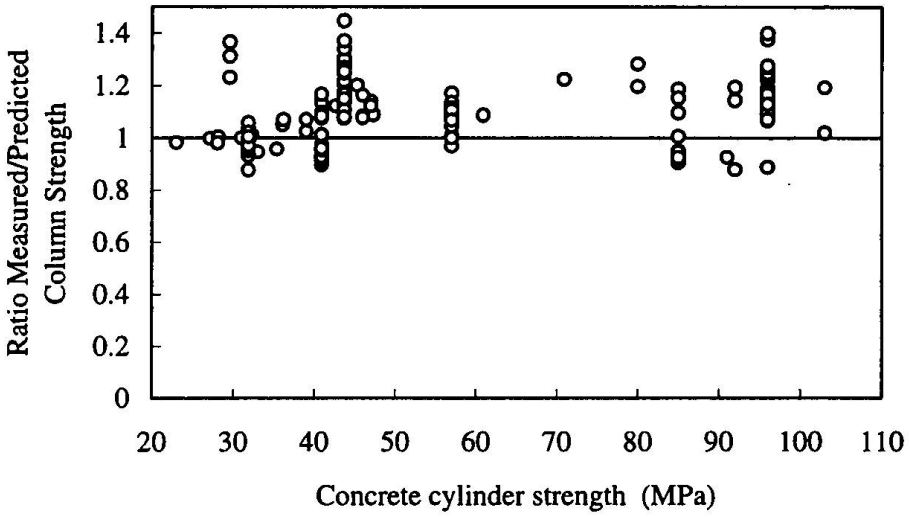

Figure 2 Column strength versus concrete strength

Acknowledgement

Assistance provided by Dr C.D. Goode towards the completion of this study is gratefully acknowledged.

References

BERGMANN R., MATSUI C., MEINSMA C. and DUTTA D. (1995), 'Design guide for concrete filled hollow section columns under static and seismic loading', CIDECT, Verlag TÜV Rheinland, pp. 68.

EUROCODE 4 (1992), 'Design of composite steel and concrete structures - Part 1.1 General rules and rules for buildings', ENV 1994-1-1:1992, European Committee for Standardization, Brussels.

GOODE C.D. (1996), Computer programme to determine the interaction diagram for a CFST cross-section, Private communication.

KILPATRICK A.E. and TAYLOR T.L. (1997), 'Comparisons Between Measured and Predicted CFST Column Strengths using EC4', Research Report No. CE 97/1, Faculty of Engineering and Surveying, University of Southern Queensland, Australia, Feb.

The Spanish Recommendations for the Design of Composite Road Bridges

Javier RUI-WAMBA
Civil Engineer
Esteyco
Madrid, Spain

José Antonio HINOJOSA
Dr. Engineer
Ministry of Public Works
Madrid, Spain

Carlos AZPARREN
Civil Engineer
Ministry of Public Works
Madrid, Spain

Summary

The Spanish Ministry of Public Works has recently published the Recommendations for the Design of Composite Road Bridges, RPX-95. The paper presents the ideas that have guided the elaboration of the Recommendations, as well as some of the main aspects of their content.

1. Introduction

Starting in the early seventies, a large number of composite road bridges of different types have been built in Spain. Considerable attention has been dedicated to the quality of the design and normally box girder sections have been used, as well as the so-called "double composite action". In 1990, the General Directorate for Highways of the Ministry of Public Works, which is responsible for most bridges in Spain, decided to fund the drafting of the Recommendations. Succesive versions of the document produced have been intensely debated by a large number of specialized engineers. The final text of the RPX-95 [1] was completed in 1995 and edited by the Ministry of Development together with the Recommendations for the Design of Steel Road Bridges, RPM-95 [2] and with the Code for Actions on Road Bridges, IAP-96 [3].

2. Guidance for producing RPX-95

The main objectives pursued in drafting the Recommendations were the following:

a) To provide a set of guidelines to be considered, although not necessarily satisfied, when designing bridges for the General Directorate for Highways.

b) To promote the quality of design and construction of composite bridges.

c) To serve as an instrument in the process of standardization, dissemination and updating of the know-how of professionals working on composite bridges.

Among the main ideas which influenced the text of the Recommendations, the following ones can be underlined:

- The bases for calculations are similar to those established in the structural Eurocodes [4].
- The philosophy of the limit states is maintained explicitly throughout the text. The verification of the serviceability limit states and that of the ultimate limit states have different objectives and are, therefore, complementary.
- It is not possible to know precisely the distribution of stresses within a structure. Thus, the calculation of stresses must be considered an instrument and not an aim in itself.
- The assumption of ideally elastic behaviours implies that the behaviour of the steel is taken to be akin to that of glass and that steel structures are therefore brittle [5], [6], [7].

- Figure 1 shows that the ultimate moment of a section decreases softly with increasing slenderness of the web. However, the rotation capacity changes abruptly when the web slenderness increases from class 1 to class 2.

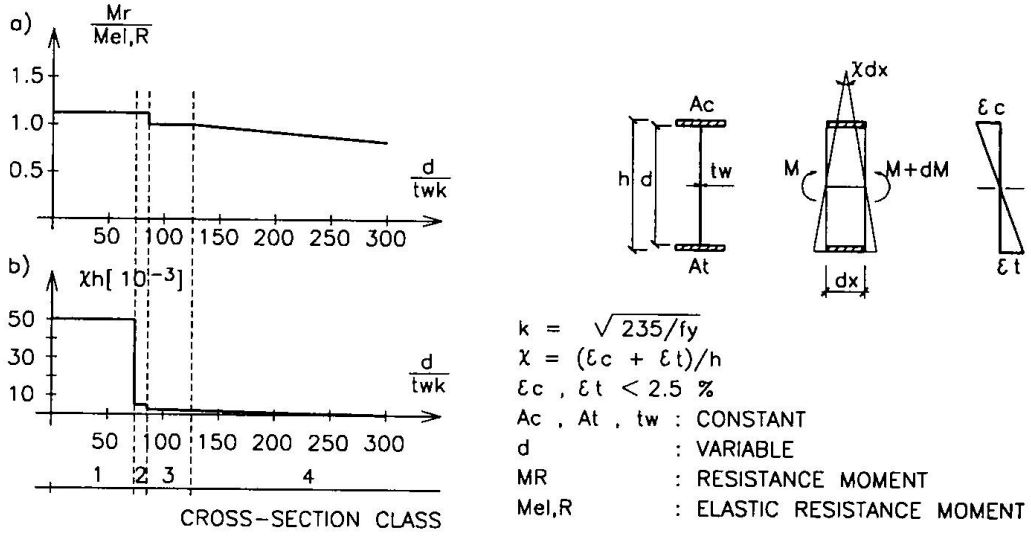

Fig. 1 Classification of cross-sections subject to bending

- It is essential, however, to guarantee a ductile behaviour. This justifies, among other things, dedicating less attention to the effects of shrinkage, creep, temperature, differential settlement of supports, seismic loads, etc. Ductility compensates some of our ignorance [8], [9].

- A good code is essential for a policy of quality which aims at progress in bridges.

- Besides the calculations, there are other aspects in the codes which are essential for achieving functionality, safety and durability: limit conditions imposed on the structural elements, durability specifications, maintenance and quality control of the design and construction processes.

- The users of the code should not use it as a substitute for thinking, neither they should consider it a collection of recipes.

- Codes also need maintenance. Every few years, the experience of their application should be assessed and, in view of the progress of knowledge, the code should be revised and updated.

3. Some characteristic aspects of the RPX-95

3.1 Structural analysis

The recommended methods of analysis are:

Method of analysis	Internal forces (ULS) Effects of actions (SLS)	Strength of sections (ULS)	Cross-section class
E/EC	Elastic (E)	Elastic with reduced section (EC)	Slender or semi-compact
E/P	Elastic (E)	Plastic (P)	All compact
E/EP	Elastic (E)	Elastic-plastic (EP)	Any cross section class
EP/EP	Elastic-plastic (EP)	Elastic-plastic (EP)	Any cross section class

The following criteria are established in order to define the mechanical characteristics of the different sections to be calculated:

Modified section denomination	Reason	To take into consideration	
		SLS	ULS
Effective section	Shear lag	YES $b_r = \psi_{el} \cdot b$	YES $\psi_{el} < \psi_{ult} \leq 2\psi_{el}$
Reduced section	Local instabilities	generally NO	YES
Equivalent steel section	Different modulus of elasticity and creep of concrete	YES	YES
Cracked section	Cracking of the concrete under tension	Depends on the tensile stress level	YES

3.2 Serviceability Limit States

3.2.1 Limit state of deformations of the structure

1st Condition: Precamber shall be the addition of the deflection caused by the permanent actions, f_p for $t = 0$ and a part of the deflection caused by time dependent effects (creep and shrinkage) evaluated for $t=\infty$. This part shall be such that the difference between the grade line calculated for $t=0$, and the functional grade line defined in the project, and the difference between the grade line calculated for $t=\infty$ and the functional grade line, are smaller than the limits of the following table:

Type of bridge	Highways	High speed road	Local roads
One isostatic span	L/2000	L/1200	L/800
Several isostatic spans	L/4000	L/2300	L/1600
Continuous	L/1500	L/900	L/600

2nd Condition: Deflections due to the "rare combination of actions" shall not affect the appearance and the functionality of the bridge.

3rd Condition: Strength criteria. Deflection due to traffic loads in the frequent combination should not exeed the limit of L/1000.

3.2.2 Limit state of the web deformation

- Stress condition for the frequent combination of actions:

$$\frac{\sigma}{1{,}1\,\sigma_{cr}} + \left(\frac{\tau}{1{,}1\,\tau_{cr}}\right)^2 \leq 1$$

- Recommendations for the minimum slenderness of the web: $f_y = 355$ N/mm^2

Zone	Beams with transversal stiffeners	Beams with longitudinal and transversal stiffeners
Intermediate supports of continuous beams (M and V,max.)	160	250
End supports of continuous and isostatic beams (M, small)	200	300
Centre span of continuous and isostatic beams (V, small)	240	350

3.2.3 *Limit state of vibrations*

- Verification of road bridges, which can be idealized as a beam, with sidewalk for pedestrians:

$$y_L \leq \sqrt{f_0}\,\frac{L \cdot f_0 \cdot 18}{2000 \cdot f_0^2} \quad (y_L \text{ and } L \text{ in meters})$$

where

f_0 frequency of the first vertical mode of vibration

y_L maximum deflection produced by a load of 10 kN/m^2 extended on the road width b and the length a = 0,9/b + 0,06 L.

3.2.4 *Limit state of local plastification*
The stresses must be checked, if it is not evident that the following limits are not exceeded:

Combination of actions	Structural steel	Structural concrete
Frequent	0,75 f_y	0,50 f_{ck}
Rare	0,90 f_y	0,625 f_{ck}

In particular it is necessary to check the stresses when ψ_{el} is below 0,6; in areas where in the ULS $\varepsilon_{max} > \varepsilon_y$ is accepted; and in singular areas with significant deformations in multiple directions.

3.3 Ultimate Limit States (ULS)

3.3.1 Ultimate bending moment, M_R, of beams
The values of M_R are established according to the σ-ε diagrams of the materials and to their deformation limits, which are summarized in the following table:

Method of analysis	Cross-section class	Deformations limits			Resisting section
		Steel		Concrete	
		Tension	Compression	Compression	
Plastic (P)	Compact	No limits	No limits	3,5 ‰	Complete
Elastic (E)	Slightly slender	4 ε_y	ε_y	$\varepsilon_c = f(\sigma_c)$	Complete
Elastic (E)	Slender	4 ε_y	ε_y	$\varepsilon_c = f(\sigma_c)$	Reduced
Elastic-plastic (EP)	Any section class	4 ε_y	1,2 ε_y	$\varepsilon_c = f(\sigma_c)$	Complete or reduced

3.3.2. Ultimate bending moment, M_R, of box girder sections
The value of M_R depends on the capacity of the compressed stiffened plate to transmit compresive forces, N_R, which is a function of the level of the deformations ε. In the Recommendations, criteria are given for determining the N_R-ε diagram of the stiffened plate [4].

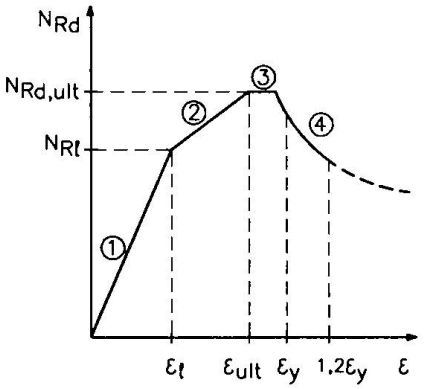

Fig. 2 Compressed stiffened plate

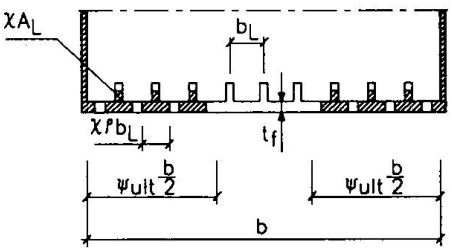

Fig. 3 Diagram N_R-ε

The maximum value of $N_{Rd,ult}$ is determined by the expression:

$$N_{Rd,ult} = \left(b_r \cdot t_f + n \cdot A_{L,r}\right)\frac{f_y}{\gamma_a}$$

where: $b_r = \psi_{ult} \cdot \rho \cdot b_L(n \cdot \chi + 1)$ and ρ is a function of $\bar{\lambda}_p = \sqrt{\frac{\chi \cdot \varepsilon_y}{\varepsilon_{cr}}}$

The Recommendations also deal with stiffened plates connected to a concrete slab:

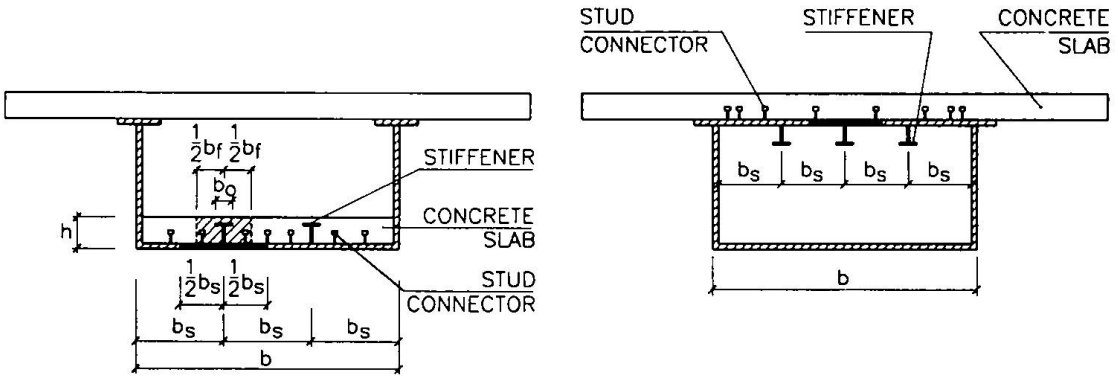

Fig. 4 Stiffened plate connected to a concrete slab

3.3.3 Interaction diagrams

The use of interaction diagrams in order to establish the safety control of sections under combined internal forces and moments has been generalized.

The influence of a simultaneous torsional moment is taken into account by reducing the ultimate bending moment and the ultimate shear force as a fuction of the external torsional moment, T_{Sd}, and the minimum value of the ultimate shear of the stiffened plate or the concrete slab, $R_{Rd,min}$:

$$M_{Rd}\sqrt{1-\left(\frac{T_{Sd}}{2A_\phi R_{Rd,min}}\right)^2}$$

$$V_{Rd}\left(1-\frac{T_{Sd}\cdot h}{A_\phi \cdot V_{Rd}}\right)$$

3.3.4 Longitudinal and transversal stiffeners

Some examples of recommended minimum conditions [6], [7]:

- T sections: $h_t/t_s \leq 30$ and $b_s/t_{bs} \leq 10$
- Longitudinal web stiffeners and transversal stiffeners of stiffened plates in box girder sections: $L_s/h_s \leq 25$
- Longitudinal stiffeners of stiffened plates: $L_s/h_s \leq 25$
- Distance, b_s, between longitudinal stiffeners of stiffened plates: $b_s/t_f \leq 120$ for tension plates, $b_s/t_f \leq 60$ for compression plates, where t_f is the plate thickness.

Besides, the necessary criteria for the evaluation of the strength capacity of the stiffeners and the required stiffness conditions are also established in the Recommendations.

3.3.5 Diaphragm in beam or box girder decks
Minimum distance between diaphragms:

- For box girders: $L_D \leq 4\,d$ (d, depth of the box girder)
- For beams: $L_D \leq 0{,}2\frac{\pi}{\sqrt{3}} b \sqrt{\frac{E}{f_y}} \approx 8{,}7\,b$ (with $f_y = 355$ N/mm^2)

where b is the width of the compressed flange.

Further, minimum stiffness requirements and criteria for evaluating the strength capacity of the diaphragms are established in the Recommendations. This is done using a simplified model consisting of virtual bars under tension or compression [6], [7], which are supposed to provide the transmission of the forces acting on the isolated diaphragm. It is also necessary to ensure that the panels between stiffeners have the necessary dimensions to permit their plastification in order to fulfil the condition of compatibility of deformations.

4. Acknowledgements

Gratitude is expressed to the General Directorate for Highways of the Ministry of Public Works; to all the Spanish engineers who collaborated in the discussions and in the elaboration of the text; to a large number of engineers from other countries who, with their publications and efforts, have contributed to the available pool of knowledge.

5. References

[1] MINISTRY OF PUBLIC WORKS. *"Recommendations for the Design of Composite Road Bridges, RPX-95"*, (1995).
[2] MINISTRY OF PUBLIC WORKS. *"Recommendations for the Design of Metal Road Bridges, RPX-95"*, (1995.
[3] MINISTRY OF PUBLIC WORKS. *"Instruction of Actions to consider in the Design of Road Bridges"*, IAP-96, (1996).
[4] EUROCODE 1 (ENV1). Part 1: *"Basis of Design"*. CEN/TC250-N105, (1994).
[5] RUI-WAMBA, J.; TANNER, P.; BELLOD, J.L.; CRESPO, P. Towards a consistent design method: *"A proposal for a new steel and composite bridge design code for Spain"*. Nordic Steel Construction Conference. Malmö, 1995.
[6] RUI-WAMBA, J. *"Research Needs for practice purpose"*. ECCS-TW68/3. 26th Meeting-Prague. April 1995.
[7] RUI-WAMBA, J.; TANNER, P. *"Design of Steel plated structures according to the Spanish Recommendations RPM/RPX-95"*. ECCS-TWG8/3. 27th Meeting. Barcelona, March 1996.
[8] MILLANES, F. *"Slenderness conditions of sections of simple and combined double actions in bridges. Criteria for the control of the limit states"*. First International Symposium of Composite Bridges. Barcelona, Nov. 1992.
[9] CORRES, H.; CALVO, S. *"Behaviour of the Section and the Structure for the Advanced Loading States. Experimental Results and Design Criteria"*. II International Symposium of Composite Bridges. Madrid, 1995.

Shear Connection for Composite Bridges, and Eurocode 4: Part 2

Roger P. JOHNSON
Professor of Civil Engineering
University of Warwick
Coventry, UK

Roger Johnson has been active in research on composite structures since 1960, and has been working on codes of practice since 1968. He is chairman of the Eurocode Sub-Committee for composite structures.

Summary

The Eurocode for composite bridges will be completed to ENV stage during 1997. Although it is required by the rules of CEN to be supplementary to Eurocode 4:Part 1.1:1994, its provisions for design of shear connection are different in many respects. They include verifications for serviceability and fatigue, one of which will often govern the spacing of connectors. These provisions are summarised, with particular reference to the effects of cracking of concrete, local concentrations of longitudinal shear, inelastic bending of beams, and relevant research.

1. Introduction

The Third Draft of the Eurocode for composite bridges [1] was circulated for comment in January 1997, after four years of work. It is expected that the Final Draft will be approved during 1997 for publication by national standards bodies as ENV 1994-2. In accordance with the rule of CEN that prohibits duplication of material, it is presented as a supplementary document to ENV 1994-1-1:1992 [2], here denoted 'Part 1.1', and is referred to here as 'Part 2'.

Part 2 has the same numbering system for Sections and clauses as Part 1.1. Each clause of Part 1.1 applies unless stated otherwise, or unless a corresponding clause labelled 'modified' or 'replaced' appears in Part 2, which also has 'additional' clauses. The drafting of Part 2 is thus constrained by the clause structure and drafting of Part 1.1 (in 1983-4). It should be possible to improve the relationship between Part 1.1 and Part 2 when their EN versions are drafted.

A brief account is given here of the differences, especially in the treatments of shear connection, between Part 1.1 and Part 2. They arise from the differences between buildings and bridges, and their loadings and exposure. The main provisions of Part 1.1 for shear connection are given next, with comments; and in outline only, because they are widely known [3,4].

1.1. Comparison of EC4:Part 1.1 with draft Part 2

Most beams in buildings are designed for uniformly-distributed loading and ultimate limit states. Except where there are cross-sections in Class 3 or 4, the shear connectors are uniformly spaced between cross-sections of maximum sagging and hogging bending moment, and their number is calculated from the difference between the longitudinal forces in the concrete slab at those sections. The rules for partial shear connection enable designers to use a connector spacing that is compatible with the profiled steel sheeting used for the floor slab. Serviceability limit states

have little influence on design, except where the degree of shear connection is so low that deflection governs; and fatigue is not within the scope of Part 1.1.

Nearly all continuous bridge beams are in Class 3 or 4. Both global analysis and the calculations of longitudinal shear per unit length use elastic theory, and design is based more on influence lines and envelopes of moment and shear, than on the simpler effects of uniformly-distributed loading. It may not be obvious which of three limit states - excessive slip in service, fatigue failure, and static failure - govern the spacing of shear connectors, so methods of verification are given in Part 2 for all three. Thin profiled steel sheeting is unlikely to be used in permanent bridges, because of the risk of corrosion. The use of partial shear connection increases slip, which in a long span may exceed the slip capacity of the connectors, so it is not within the scope of Part 2.

Beams that are of non-uniform section, or curved in plan, and sets of closely-spaced beams, perhaps on skewed supports, are common in bridges, but not in buildings. Provision has also to be made in Part 2 for structural systems such as tied arches, half-through bridges, and trusses, and for the use of prestress and double composite action.

Part 2 has to be consistent with Eurocode 2:Part 2 for concrete bridges [5], in which the clauses on fatigue and on creep, shrinkage, and cracking of concrete are more complex than in EC2:Part 1.1. The relevant provisions of EC4:Part 2 are simpler than in earlier drafts, especially in respect of tension stiffening in cracked concrete. Experience of its use in trial designs should lead to further simplifications, such as the definition of more situations where specific checks (e.g., on fatigue in reinforcement) are not required.

2. Properties of shear connectors

The types of shear connector covered in Part 2 are as in Part 1.1, except that welded reinforcing-bar anchors are excluded. The resistances to static load are unchanged, but for studs are limited to a maximum diameter of 22 mm. (More data are needed on properties of 25-mm studs). Where failure of a connector clearly occurs in a single material (e.g., steel, concrete, or a weld) the usual safety factor γ_M for that material is used. The failure of a stud connector arises from interaction between steel and concrete, so a single factor γ_M (= 1.25) is used, based on calibration. Thus, the ratio of design resistance at ultimate limit states to characteristic resistance P_{Rk} depends on the type of connector used.

For the serviceability limit state of maximum stress, the force per connector is limited to $0.6\,P_{Rk}$. The intention is to avoid inelastic behaviour and 'excessive' slip, for which there is no simple definition. The ratio 0.6 is based mainly on existing practice.

For all types of connector except studs, the resistance to fatigue is governed by welds that can be verified using Eurocode 3 for steel structures. There is no consensus in the literature on the fatigue resistance of welded studs. A recent study [6] of reports on 211 push tests found recommended values of the exponent m ranging from 5 to 11.5. At least seven different types of test had been used, and the results came from at least four different statistical populations.

It became clear that in design to Part 2, fatigue loading would not cause loads per connector exceeding $0.6\,P_{Rk}$, and that the influence of strength of concrete on fatigue failure could then be neglected. (This is not done in the UK Bridge Code, BS 5400, where fatigue resistance is a

function of static resistance, which for many connectors is influenced by the strength of the concrete). This assumption enabled the fatigue resistance of studs to be defined by an *S-N* line, as for other welded details. Based partly on [6], the fatigue resistance of a stud of diameter d has been defined, in N, mm units, by

$$N [\Delta P_R / (\pi d^2 / 4)]^8 = 10^{22.123}, \quad (1)$$

where N is the number of cycles to failure, for shear force range ΔP_R per stud. This is a characteristic value, for use with $\gamma_M = 1.0$. It gives the fatigue strength in shear as $\Delta\tau_c = 95$ N/mm^2, for the reference value $N = 2 \times 10^6$. For lightweight concrete, this value is scaled down in proportion to the density. A tri-linear interaction expression is given for fatigue verification where a shear connector is welded to a steel flange in tension; and in this situation, the diameter of a stud connector is limited to 1.5 times the thickness of the flange. It has not been possible to implement recent research on the influence of cumulative fatigue damage on static resistance [7].

During construction, shear connectors may be subjected to shear force before the surrounding concrete has reached its design strength. It is recommended in Part 2 that the placing of fresh concrete should be so planned that this does not occur where the cylinder strength of existing concrete is less than 20 N/mm^2, at which strength connectors should be asssumed to become effective.

3. Determination of longitudinal shear

In principle, shear connection is designed for a shear flow, v, that is the rate of change of the longitudinal force in either the steel or the concrete element of a composite member, using the maximum value at each cross-section, and considering all design combinations and arrangements of actions. The usual basis is the design envelope of transverse shear (i.e., vertical shear V in a horizontal member) and use of the well-known elastic theory that gives $v = VA\bar{y} / I$. To apply this principle, approximations are necessary. Some of these are now given.

Where account is taken in global analysis both of the effects of cracking of concrete and of tension stiffening, the second moment of area I and the associated section properties A and $\bar{y}$ in the equation above may, in cracked regions, be calculated for the cracked concrete section, including the effects of tension stiffening. In all other situations, the 'uncracked' properties should be used. The 'cracked' properties neglecting tension stiffening may not be used, because this underestimates the forces on connectors, especially in structures such as tied arches where the deck is not prestressed. (This option of using the cracked section, which reduces the number of connectors required, is not given in the UK Bridge Code).

Generally, longitudinal slip is ignored, but there are many situations where it is necessary to take advantage of the effects of slip on local concentrations of longitudinal shear. Design rules, mostly based on finite-element analyses, are given in Part 2 for the following situations:

- sudden change of cross-section of a composite member (empirical),
- isostatic effects of temperature and shrinkage near an end of a composite member (based on the UK Bridge Code),
- application of a concentrated longitudinal force; e.g., by a prestressing tendon or a web member in a truss or frame (based on reference [8]).

This last rule is illustrated in Figure 1(a), which shows a prestressing force with design value F_d applied to the slab at lateral distance e_d from the shear connection. The proportion of F_d that is transferred to the steel section, V_ℓ, is determined by conventional elastic analysis of the composite section. The distribution of design longitudinal shear v_d may be assumed to be trapezoidal, as shown, with a maximum value

$$v_{d,max} = V_\ell / (e_d + b_{eff}/2)$$

where b_{eff} is the effective width of the concrete flange, as used in the global analysis. For stud connectors, this distribution may be replaced by a rectangular one over the length L_v.

For the trapezoidal distribution, the compressive force in the slab caused by the prestress increases from zero to $F_d - V_\ell$ over a length L_v $(= e_d + b_{eff})$ as shown in Figure 1(b). The maximum tensile force in the slab is given by

$$\Delta N = v_{d,max}\, b_{eff} / 4.$$

The distribution of longitudinal shear caused by several forces F_d is obtained by summation. Similar rules are given for the longitudinal force applied to the concrete element of a flange by a web member in a truss or frame.

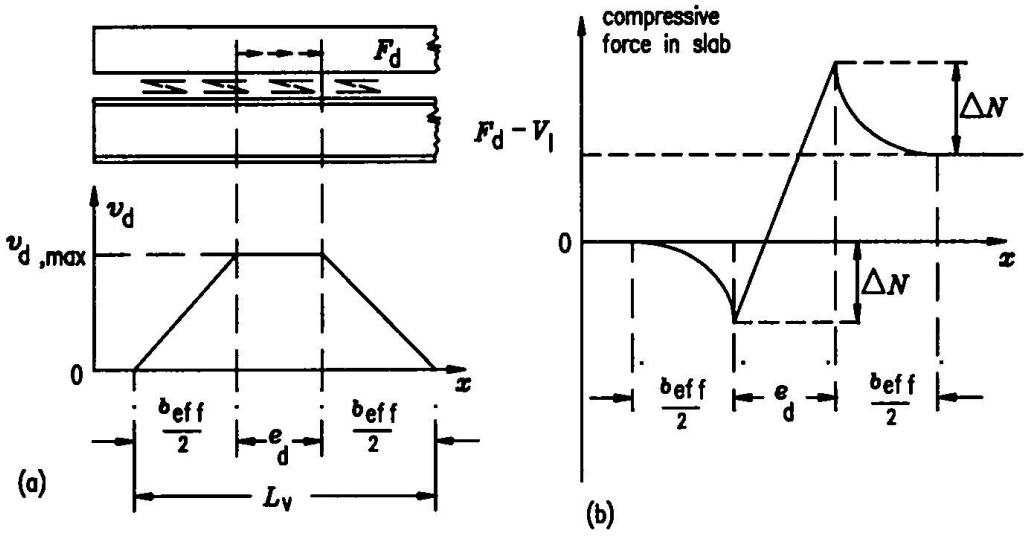

Fig. 1 Distribution of longitudinal shear force along the interface

The preceding elasticity-based methods are applicable for all limit states, but are unconservative for longitudinal shear near a region of a member in slenderness Class 1 or 2, where resistance to bending is based on plastic section analysis, and can exceed the elastic resistance by 30% or more. After many trials, a design rule for this situation was found, based on the treatment of partial shear connection in Part 1.1. In a midspan region, its use may not lead to the provision of more connectors, because each check is for a specific bending-moment distribution, rather than for an envelope, and also because the separate check for fatigue may govern.

4. Fatigue of shear connectors

Application rules are given in Part 2 only for fatigue design using nominal stress ranges based on fatigue load models (FLM) 3 for road bridges and 71 for railway bridges, as defined in Eurocode 1:Part 3 [9]. For road bridges, the FLM3 vehicle applies eight wheel loads of 60 kN within an area 8.8 m long and 2.4 m wide. For stud connectors, the range of shear stress per stud is determined for its passage across the bridge in the most critical lane, and multiplied by a damage equivalence factor $\lambda_{v1}\,\lambda_2\,\lambda_3\,\lambda_4$, using tabulated λ factors that are functions of the length of the influence area, the specified traffic and design life of the bridge, and the slope of the *S-N* line for fatigue strength. These factors are as given in Eurocode 3, for both highway and railway loading, except for λ_{v1}, which differs from λ_1 in Eurocode 3, and is given in Part 2. This is to allow for the exponent 8 in equation (1), which is higher than for the welded details covered by Eurocode 3.

The result is $\Delta\tau_E$, the damage-equivalent constant-amplitude shear stress range for 2×10^6 cycles, and the verification is

$$\gamma_{Ff}\,\Delta\tau_E \leq \Delta\tau_c / \gamma_{Mf},$$

where $\Delta\tau_c$ is given above, and γ_{Ff} and γ_{Mf} are the partial safety factors for fatigue.

5. Which limit state governs the spacing of shear connectors ?

For simplicity, the methods of analysis given in Part 2 are, wherever possible, the same for all limit states. Where alternatives are given, as for the treatment of cracking of concrete, the simpler one is usually the more conservative, and is likely to be used in the design of small and simple bridges.

This similarity of methods enables a rough comparison to be made, for highway bridges, between the numbers of stud connectors required for the serviceability and ultimate limit states, n_s and n_u, respectively. For most permanent and traffic actions, $\gamma_F = 1.35$, so the ratio of action effects (SLS/ULS) is $1/1.35 = 0.741$. For studs, the ratio of limiting force per connector is $0.6\,P_{Rk}$ to $P_{Rk} / 1.25$, which is 0.75. On this basis, $n_s / n_u = 0.741/0.75 = 0.99$.

It is not as simple as this, for many reasons, such as the differences between the load combinations for the two types of limit state; but the conclusion that ultimate and serviceability criteria give similar numbers of connectors is supported by the design exercises done so far. If fatigue governs, it is most likely to do so in a region near midspan.

5. Miscellaneous

Reference is made here to some aspects of Part 2 that do not belong under earlier headings.

There is an application rule that, adjacent to cross frames and vertical stiffeners, design should be such that no significant uplift forces are applied to the shear connection by rotation of the deck slab about a longitudinal axis. It has not been possible to give specific guidance on a problem that often leads to discussion between designers and checkers but, it is believed, has never been implicated in a failure.

For the design of transverse reinforcement near shear connectors, the only significant change from Part 1.1 is that the design shear strength of the concrete, τ_{Rd}, is taken as zero in regions where the calculation of longitudinal shear is based on a cracked cross-section (and so is much lower than if the uncracked section had been used).

The preceding rule is an example of many clauses where there is an implied assumption that composite action occurs in one flange only of the member. Where there are two composite flanges, the rule on τ_{Rd} is intended to apply only to the flange in tension, but that is not stated.

6. Closure

The new design methods summarised above refer to and are consistent with the ENV (preliminary) versions of Eurocode 1:Part 3, Eurocode 2:Part 2, and Eurocode 3:Part 2. All these codes need extensive trial use in practice, over the 3-year ENV period that should begin in 1998. This should enable improved EN versions to be drafted and, it is believed, some methods to be further simplified.

The author acknowledges with thanks the value of many discussions on this subject with the other members of the Project Team for Eurocode 4:Part 2: M J. Raoul and Professors G. Hanswille, B. Johansson, M. Mele, and F. Tschemmernegg.

References

1. ENV 1994-2, 'Eurocode 4: Design of composite steel and concrete structures, Part 2: Bridges'.Third Draft. Circulated to National Technical Contacts, January 1997.
2. DD ENV 1994-1-1, 'Eurocode 4: Design of composite steel and concrete structures, Part 1.1: General rules and rules for buildings', British Standards Institution, London, 1994.
3. Johnson, R.P. and Anderson, A. 'Designers' handbook to Eurocode 4:Part 1.1'. Thomas Telford, London, 1993.
4. Stark, J.W.B. 'EC4: Serviceability, shear connection, and composite slabs'. *Reports*, **65**, 223-231, Int. Assoc. for Bridge and Struct. Engrg, Zurich, 1992.
5. ENV 1992-2, 'Eurocode 2: Design of concrete structures, Part 2: Concrete bridges'. CEN, Brussels, 1996.
6. Yuan, H. 'Fatigue strength of stud shear connectors'. Technical Paper JB 44, Project Team for Eurocode 4:Part 2, January 1995.
7. Johnson R.P. and Oehlers D.J. 'Integrated static and fatigue design or assessment of stud shear connections in composite bridges'. *The Structural Engineer*, **74**, 14, 236-240, 16 July, 1996.
8. Ivanov, R.I. 'Loading of the shear connection of composite beams due to prestress'. MSc thesis, University of Warwick, September 1996.
9. ENV 1991, 'Eurocode 1: Basis of design and actions on structures, Part 3: Traffic loads on bridges'. CEN, Brussels, 1994.

A Draft Design Code for Steel-Concrete Composite Slabs in Japan

Shigeyuki MATSUI
Dr. and Prof. of Civil Eng.,
Osaka University,
Osaka Japan

Shinich HINO
Dr. and Assoc. Prof. of Civil Eng.,
Kyushu University,
Fukuoka Japan

Koji OHTA
Senior Manager
Nippon Steel Corporation,
Tokyo Japan

Isao SHIMIZU
Section Chief
Miyaji Iron Works Co.LTD.,
Tokyo Japan

Hideo IKEDA
Section Chief
Japan Bridge Corporation,
Osaka Japan

Yoshihisa TAKEDA
Section Chief
Kawada Industry Co.LTD.,
Nagoya Japan

Summary

Design codes of the composite decks based on a limit state design method which are proposed by the Committee on Composite Structures in JSCE are introduced . There are many types of composite decks. But, the essential types are two such as concrete encased type and steel plate concrete composite deck. This paper reports concretely the design codes about the latter steel plate concrete composite decks.

1. Introduction

Reinforced concrete slabs (hereafter RC slabs) have been used for the decks of highway bridges with their lower cost and easier construction than other types of decks. But, since about 1966, heavy deterioration problems have occurred due to repetitions of heavy traffic loads and penetration of rain water. Therefore, development of durable decks has been required and some prestressed slabs, concrete filled steel grillage decks and steel plate concrete composite decks were developed. These tendencies are accelerated by recent decreasing of field workers and new demands to built bridges more economically. Composite decks seem to be favorable decks because they can be fabricated by semi-prefabrication. Also they will become more lighter than RC slabs and more durable. Various types of composite decks have been developed or proposed. But until now, a rational design method was not prepared for those composite decks except the one for grating slabs.
The task committee for composite structures(chairman is Prof. H.Nakai) of the sub-committee for ultimate strength, the committee of steel structures, JSCE has been discussing for these 3 years to propose the design codes for composite structures. Last year, the draft of the codes were completed and now the draft is under checking. This paper is introducing a part of the draft of composite decks, thus, about steel plate concrete composite deck and the detailed basic data are described.

2. Outline of the Draft Codes for Composite Decks

Table 1 shows the contents of the design codes for composite decks. In Chapter 1~6, common requirements for all kinds of composite decks are codified. The decks have to be checked with three limit states such as the ultimate limit state, the serviceability limit state and the fatigue limit state. When a deck is used for highway bridges, the ultimate strength of the deck will be very large comparing to the design wheel load and therefore the check

Table.1 Contents of the draft code for composite decks

Chapter 1. General
Chapter 2. Materials
Chapter 3. Analysis
Chapter 4. Strength and Quality of Materials
Chapter 5. Verification for Limit States
Chapter 6. Details of Composite Decks
Chapter 7. Design Robinson Type Composite Deck for Highway Bridge
Chapter 8. Design Grating Deck Slab for Highway Bridge

for the ultimate limit state can be neglected.
Fatigue limit state, however, should be checked, because the deck on highway bridge is subjected to high cycles of loading of wheel loads. Under running wheel loads, the fatigue failure modes can be presumed to be different from the ones obtained by the ordinary pulsating loading method. Until now, the fatigue characteristics under running wheel loads of only the two types of the composite decks were obtained and proved. Therefore, considering the different fatigue failure modes, special design codes for the steel plate concrete composite decks (Robinson type deck) and the concrete encased steel grille slabs (grating slabs) for the design of highway bridges are prepared in Chapters 7 and 8.

3. Design Codes for Steel Plate-Concrete Composite Decks

3.1 Features of Steel Plate-Concrete Composite Decks

Fig.1 shows an essential type of steel plate-concrete composite decks named as Robinson deck. Studs are used for the shear connectors between the steel plate and concrete slabs. Steel plate acts as scaffolding of concrete when casting concrete. After hardening of concrete, the steel plate will develop a great bending rigidity due to composite action combined with concrete as the reinforcements in RC slabs. They acts as tensile members. Also, there are some cases that the steel plates are stiffened by ribs at bottom surface or top surface. When the ribs are arranged, as they act as shear connectors, the number of studs can be reduced.

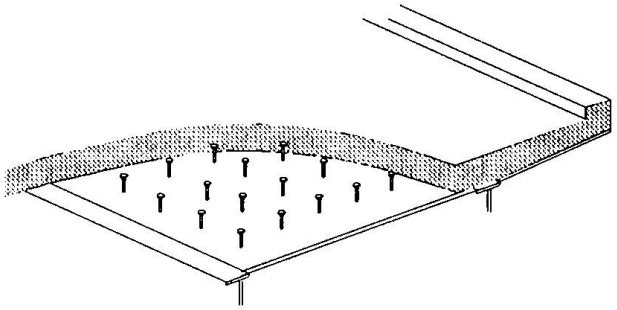

Fig.1 General view of steel plate concrete composite deck

When the deck is applied on the multi-girder bridges, the deck becomes a continuous deck and on the supporting girders negative moments will develop. To resist for the negative moment, near the top surface appropriate numbers of reinforcements should be arranged. As shown in Table 2, there are several actual bridges having the composite slab constructed and the almost slabs are designed with the design codes for RC-slab. In those cases, the steel plates act as top flanges of the supporting girders simultaneously.

Table.2 Actual bridges with composite decks

Bridge Name	The examples of the composite slab with stud	Slab span length
Nishinagahori Ramp Bridge	Hanshin express way public corporation	1.775m
Katamachi Bridge	Osaka city office	2.625m
New Osaka Castele Bridge	Osaka city office	1.700m
Tanaka Bridge	Asago village office	3.000m
Kanari Bridge	Asago village office	3.000m

3.2 Bending Moments to Design the Cross Section of the Deck

Bending moment distributions of decks under considerable severe loading of wheel loads are analyzed by FEM Analysis. Then, the maximum bending moments acting orthogonal directions in a deck were plotted and investigated with the span length as shown in Fig.2. The analytical results can be said to have a linear relation to the span length. In the large span region over 5m, the effect of the front axle weights becomes large and has to be considered on the maximum bending moments for design.

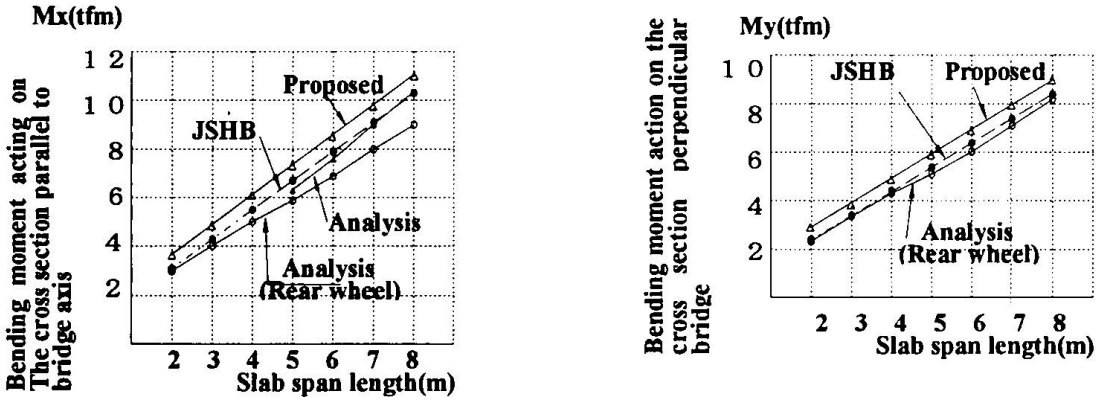

Fig 2. Design bending moments for steel plate concrete composite decks

By covering the maximum bending moments and giving some safety margin to the analytical results, bending moment formulae can be proposed. The upper straight lines are the formulae. Those are given with some safety margin from 20%(for slab span 2m) to 8% (for slab span 8m). The decrease of the safety margin as the span length becomes large is due to the decrease of probability of simultaneous loading of heavy wheels as the design

Table.3 Bending moments formula for continuous steel plate concrete composite decks.

Deck System	Aimed Section	Span Length(m)	Bending Moment	
			On cross section parallel to bridge axis	On cross section perpendicular to bridge axis
Simple span	Span center	2≦L≦8	+(0.114+0.144)×P	+(0.095L+0.098)×P
Continuous deck	Span center	2≦L≦8	+80% of simple span	+80% of simple span
	On support		-80% of simple span	
Cantilever	On support	0<L≦1.5	-PL/(1.3L+0.25)	
	Free side			+(0.15L+0.13)×P

L ; Slab span
P ; Wheel load(=10t)

load.
The proposed bending moment formulae are the essential bending moments for a one-way slab of single span deck. Generally, the decks, however, will be continuous plates over multiple number of girders. Therefore, the formulae should be modified available to continuous decks. Table 3 is the final proposal about the bending moments for steel plate concrete composite decks.

3.3 Verification for Limit States

Essentially, for the decks of highway bridges the verification for the ultimate strength may be neglected because the ultimate strength becomes very large such as 8 to 10 times of the design wheel load. Never the less, deterioration will occur due to fatigue by running wheels and environmental effects. Therefore, for the design of decks a working stress method or an allowable stress method seems to be appropriate. But, this design method had to be expressed by an ultimate strength format. Here, the allowable stresses were set as 1/3 of compressive strength for concrete and 1/1.7 of yielding stress for steel plate. Then, by multiply the factors 3 or 1.7 to the bending moments, the intended cross section can be verified by the compressive strength for concrete surface and the yielding for the tension side steel plate.
Verification for fatigue on the main materials of concrete and steel plate can be neglected when the above mentioned design procedures is applied.

3.4 Minimum Requirements for Cross Sections

3.4.1 Steel plate thickness

For the decks of under 3m span length, the thickness of steel plate seems to be enough by 6mm. In the existing decks 4.5mm plate were frequently used. The thickness can be decided by the stress state. However, some problems are there such as fatigue failure of the steel plate at the welding parts of jointing or the places of stud welding and deformation by welding. Also, in Japan to obtain those thin steel plate is little bit difficult than normal thickness ones. Furthermore, treatment at the factory is more easy for the normal thickness plate than the thin ones. Considering the above mentioned problems and the margin for corrosion, the minimum thickness is decided as 8mm for the composite decks. For the wider

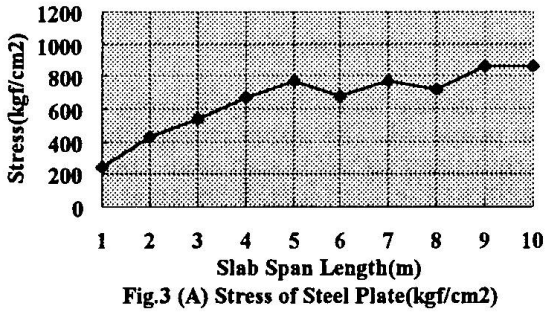

Fig.3 (A) Stress of Steel Plate(kgf/cm2)

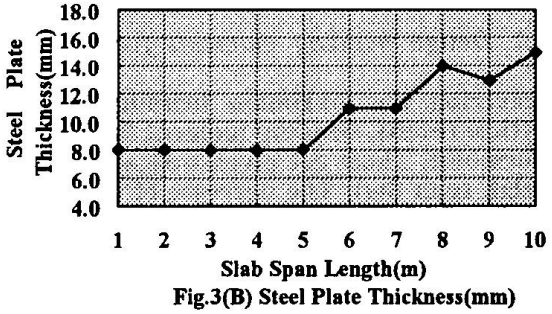

Fig.3(B) Steel Plate Thickness(mm)

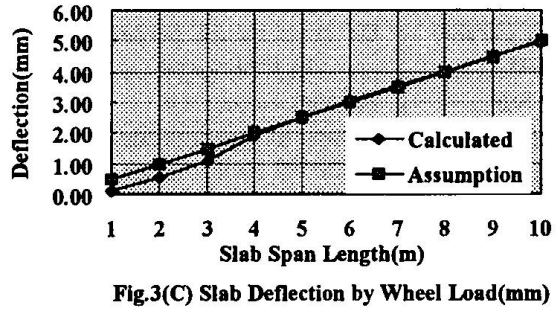

Fig.3(C) Slab Deflection by Wheel Load(mm)

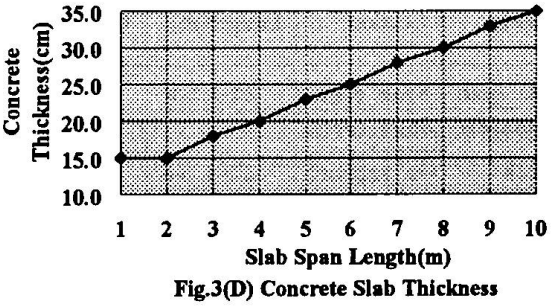

Fig.3(D) Concrete Slab Thickness

Fig.3 Calculation results of steel plate concrete composite decks.

deck than 6m span length, the steel plate thickness becomes more thick than 8mm. Fig.3(A) and Fig.3(B) are shown the relations of the steel plate stress and required steel plate thickness to the span length respectively.

3.4.2 Concrete slab thickness

The concrete slab thickness on the steel plate can be reduced than the ones of ordinary RC slabs due to composite action with steel plate. This idea is supported with many experimental tests. However, in the case that a remarkable thin slab is used, deflection becomes large inducing some local deterioration of concrete and some harmful cracks occur on the top surface due to repetition of torsional bending moment. The cracks becomes penetration crack through full depth by joining the both cracks from the bottom and top surface which decreases the bending rigidity of the deck. Also, when the water penetration occurs into the cracks from top surface, the concrete will show early deterioration by fatigue.

Therefore, a limited thickness of concrete layer on the steel plate is required. From experimental knowladges, concrete thickness seems to be appropriate when the deflection under design loads is kept less that L/2000, where L is slab span length. When the concrete thickness is given likes the Fig.3(D), the deflection becomes under the assumption. In the draft, the thickness is decided as the following equation;

$$hc\ (cm) = 2.5 \times L\ (m) + 10$$

The minimum thickness was set to 15cm by the construction performance.

Fig.3(C) and Fig.3(D) are shown the relations of slab deflection and the concrete slab thickness to slab span length, respectively.

3.5 Design of Studs

3.5.1 Fatigue tests with wheel Running Machine

The authors have carried out many fatigue tests on the steel plate-concrete composite decks with the Wheel Running Machine. The machine is to give a running wheel load on the specimen as shown in Fig. 4 . It was developed to simulate the running wheel loading which was found out the most important factor of the fatigue of decks on highway bridges.

From the fatigue tests of the composite deck, the predominant fatigue failure mode was detected as shear-off failure of stud as shown in photo.1. When the deck is loaded by pulsating load on a fixed point, the failure mode will be a break of steel plate initiated at the welding points of studs. The difference of fatigue modes is caused by the difference of moving or not moving of wheel loads.

Under the running wheel load, the studs are subjected to rotating shearing forces and then the shear-off failure occurs. The authors are thinking the fatigue test method by the wheel running machine is favorable one by simulating the running of vehicles. Therefore, in the draft, the authors have recommended to do fatigue design for the studs considering shear-off failure of studs. The codes gives how to calculate the shearing force on studs and the limitation shear stress to avoid the fatigue failure.

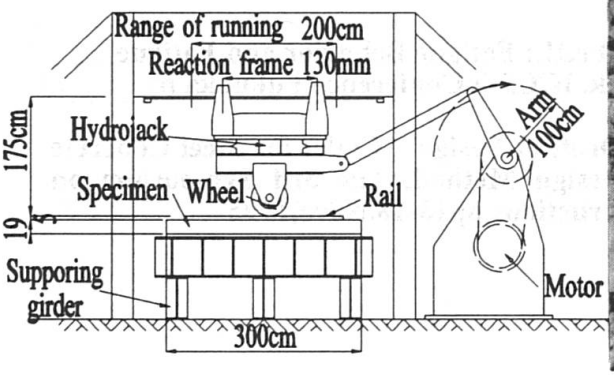

Fig.4 Wheel running machine

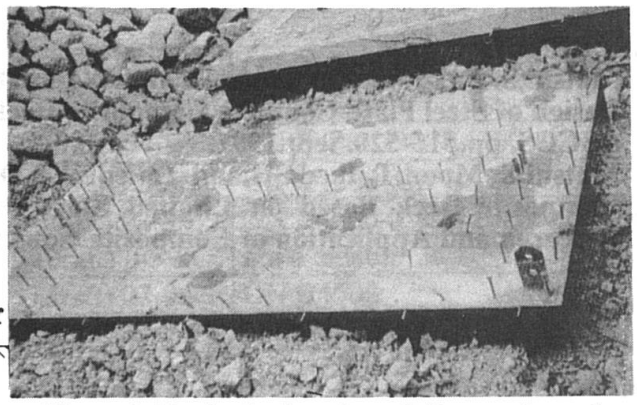

Photo.1 Typical shearing failure of studs

3.5.2. Allowable shearing stress of studs

As mentioned in the above, the studs fail by shear-off under running wheel load. The fatigue strength is evaluated by the shearing stress as shown in Fig.5. In the figure, the S-N data of push-out test method are presented simultaneously. Comparing the present data with the S-N data, the present fatigue strength seems to decrease to only 30-40% of the one of the push-out test. The reduction is very remarkable. It seems due to rotating shear force on studs by running of wheel.

To investigate more quantitatively the fatigue strength, the authors have developed a quite original fatigue device to give rotating shear force on a stud and have carried out many fatigue tests. The test results are also plotted by the black circles. The data situate little bit lower side than the data obtained from deck specimens(white circles). So, it can be understood that when the data obtained from single stud test are applied for the design, the result becomes conservative. On the other hand, the data obtained from the single stud have somewhat large scatterness and the slope of the mean S-N curve is very flat. So, through much discussion the constant shear stress of 5kg/mm2 is recommended as the allowable stress to prevent fatigue failure of studs.

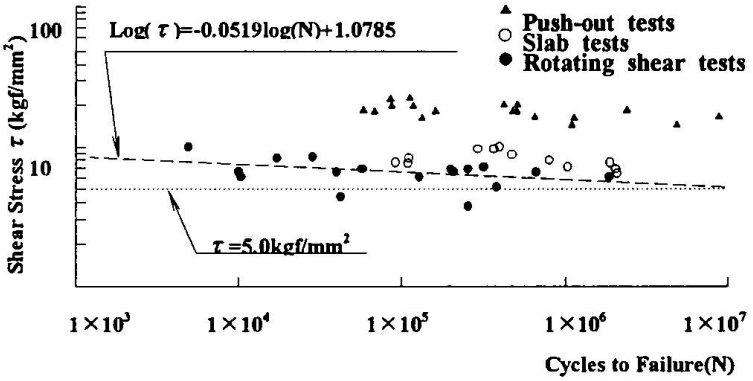

Fig.5 S-N results of studs (φ16)

4. Concluding remarks

In Japan, another types of shear connectors are developed. For those shear connectors or decks, the fatigue design method has to be investigated by another research works. At the time, the fatigue test method described here seems to be available. When this composite slabs is fabricated by precast type, the jointing between precast slabs becomes as a big problem. Various type of joints can be imagined but their durability should be checked by the fatigue tests.

REFERENCE

1) **Matsui,S. Fukumoto,Y. Moon,T. and Watanabe,H,: Fatigue Behavior and Fatigue Design of Steel Plate-Concrete Composite Deck, ICCS-3 Conference Fukuoka by ASCCS, pp.515-520.Sept.1991.**
2) **Matsui,S. Moon,T. Ikeda,H.and Takeda,Y,: Draft of Design Codes for Steel Concrete Composite Deck Based on Limited State Design Method, The 3rd Symposium on Research and Application of Composite Constructions,pp13-18,Nove,1995**

Composite Bridges in View of Existing Standards and Eurocode

Herbert POMMER
Civil Engineer
Waagner Biro AG
Vienna, Austria

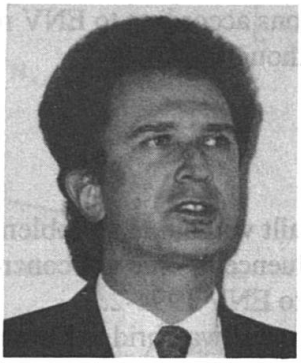

Herbert Pommer, born 1956, received his civil engineering degree at TU Wien in 1980 employed at Waagner Biro AG in the bridge department since 1981

Summary

For the design of composite bridges some comparative calculations between Austrian standards and Eurocodes have been made. Simple span and continuous span railway bridges, a simple span truss railway bridge and a cable-stayed road bridge have been examined. The results and the major interesting aspects for the practical use of ENV 1994-2 are presented in this paper.

1. Introduction

Austrian standards for the design of composite railway bridges are not compatible with load specifications and steel structure specifications. There are no standards for composite railway bridges available. However, several bridges have successfully been built with the knowledge and common sense of engineers in the last few years.
In Austria prestressing without tendons is mainly used, e.g. erection methods like lowering the concrete slab at supporting points.

2. Standards

The main Austrian standards for the design of composite bridges compared with Eurocodes are indicated below.

	Eurocode	**ÖNORM** (Austrian standard)
General design	ENV 1994-2 (draft) 07-96	ÖN B4500
Steel Structure	ENV 1993-2-2 (draft) 04-96	ÖN B4600 ÖN B4300
Concrete slab	ENV 1992-2 10-95	ÖN B4200 ÖN B4700
Fatigue in steel construction	ENV 1993 2-2 (draft) 04-96	ÖN B4600-3 ÖN B4300-5
Fatigue in concrete slab	ENV 1993-2-2 (draft) 04-96	not available
Composite road bridges	ENV 1994-2 (draft) 07-96	ÖN B4502
Composite railway bridges	ENV 1994-2 (draft) 07-96	not available

3. Loads

For a critical examination of standards for bridges the design regulations as well as the load specification have to be compared.
The different way of calculation of load actions according to ENV regulations does not bring about a significant influence on the design, though.

4. Simple span bridges

Simple span composite bridges have been built without any problems in the last twenty years. As a simplification for small bridges the influence of creep of concrete may be taken into account by use of modular ratios according to ENV 1994-2.
The comparative calculation for a simple span railway bridge has shown that there are only minor differences between ÖNORM and Eurocode.

5. Continuous span bridges

There are various methods to minimise cracks in the concrete. Prestressing by tendons has been the main method in Germany for many years. In Austria prestressing methods by lowering the composite girder are used.

5.1 Calculation without tension stiffening effect

This method is used in ÖNORM and DIN and can also be applied according to ENV 1994-2.

5.2 Calculation with tension stiffening effect

In tension members in composite beams the stiffness and the conrete tensile strength can be taken into consideration. A comparative calculation for a continuous span railway bridge with variably high beams shows that there are great differences depending on whether tension stiffening effects have been taken into consideration or not.

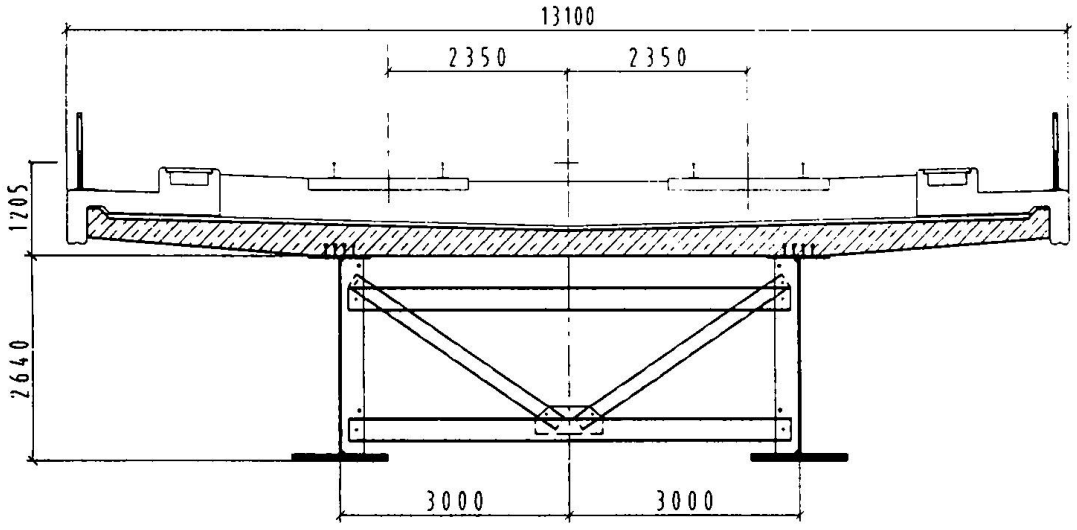

Fig. 1 Cross section of railway bridge near Melk/Austria

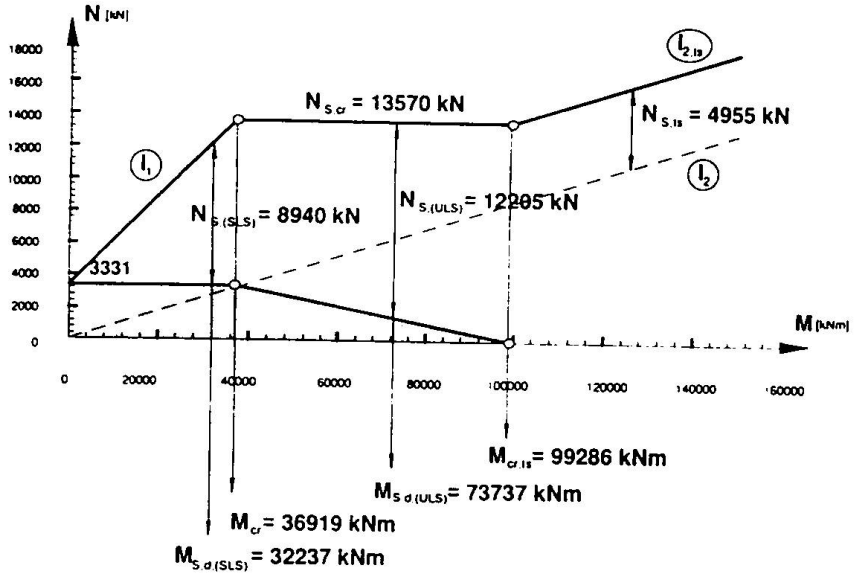

Fig. 2 N_s-M Diagram of the hogging bending moment at the internal support

Region (a) gives the behaviour of the uncracked section, region (b) the behaviour in the stage of initial crack formation and region (c) the behaviour in the stage of stabilised crack formation. Comparative calculations have shown that the consideration of the tension stiffening effect according to ENV 1994-2 will result in an economization of steel quantities by about 10 % in contrast to ÖNORM.

6. Trusses with concrete slabs

There are no regulations in ÖNORM for calculating composite truss bridges. ENV 1994-2 allows an economical calculation according to Annex L. Detailed examples are given in [9].

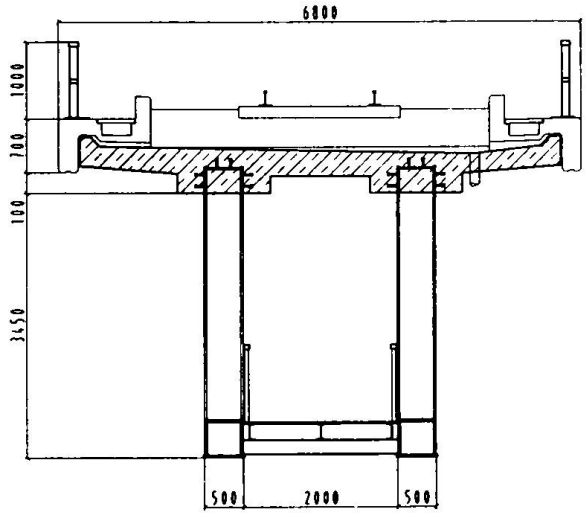

Fig. 3 Cross section of railway bridge Siemensstraße/Austria

7. Tension members in bowstring arch- and cable-stayed bridges

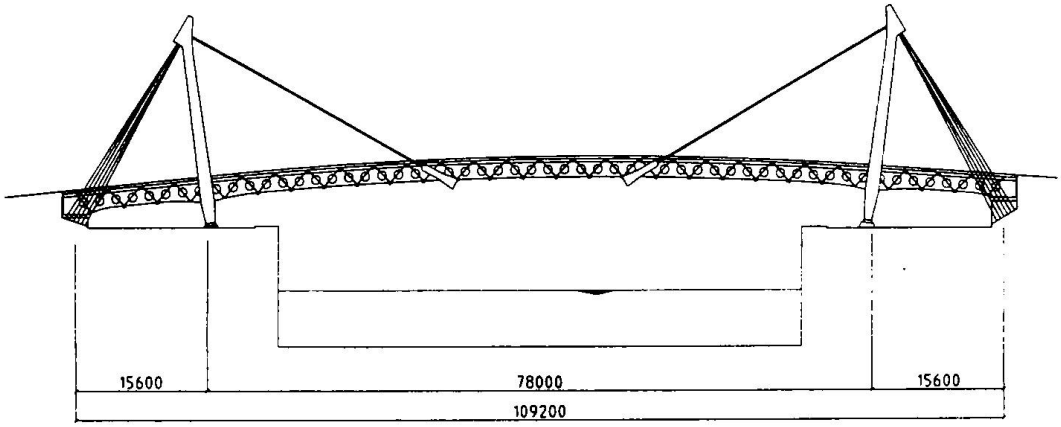

Fig. 4 View of the cable-stayed road bridge Freudenau/Austria

In ÖNORM there are no regulations if the complete or larger parts of the conrete slab are under tension. The application of ENV-1994-2 to tension members in concrete slabs offers the possibility to calculate composite bowstring arch- and cable-stayed bridges.

8. Serviceability limit states

In ENV 1994-2 serviceability limit states cover limitation of stress, crack and decompression control, deformation and vibration.

8.1 Classification for design criteria

According to ENV 1994-2 a bridge or parts of the bridge have to be classified into design categories. The category has to be indicated in the project specification.

	Combination of actions for the verification of:	
Category	Decompression	Crack width
A	infrequent	--
B	frequent	infrequent
C	quasi permanent	frequent
D	--	frequent
E	--	quasi permanent

Existing road- and railway bridges which were built according to Austrian standards comply with category C of ENV 1994-2.
Categories A and B can only be fulfilled with prestressing by tendons.

8.2 Control of cracking

In ÖNORM regulations of crack control and minimum reinforcement are given for road bridges only. In ENV 1994-2 clear regulations are given for both road- and railway bridges. These regulations are stricter than those of ÖNORM B4502. Due to the advantages of considering the tension stiffening effect it is justified to increase the reinforcement quantity, however.

8.3 Deformations

According to ENV 1994-2, as a simplification the effective sections for calculation of deformations may be taken from sagging moment area of the global analysis over the whole length of the bridge. The tension stiffening effect may be included in the calculation of the deformations.

9. Ultimate limit states

Composite bridges are supposed to be proportioned in such a way that the basic design requirements for the ultimate limit states are satisfied. As a simplification the influence of creep of concrete may be taken into account by use of modular ratios. According to ENV 1994-2, in sections where the concrete slab is assumed to be cracked, the primary (isostatic) effects due to shrinkage may be neglected in the calculation of secondary (hyperstatic) effects.

10. Ultimate limit states for shear connections and fasteners

Comparisons indicate that welded stud shear connectors calculated according to ENV 1994-2 can carry 45% more shear load than those calculated according to ÖNORM. The influence of fatigue of shear connectors on railway- and road bridges have to be taken into account.

11. Fatigue in the steel structure

In contrast to ÖNORM B 4600-3 the regulation of ENV 1993-2 requires more steel consumption. In the past, fatigue in the steel structure of composite bridges has not been decisive for dimensioning. Comparative calculations for continuous span bridges result in an increase in the amount of steel by 10%, if designed according to ENV.

12. Fatigue in the concrete slab

In the past no fatigue regulations for the concrete slab have been applied. The fatigue strength of reinforcing steel and prestressing steel should be taken into account according to ENV 1992-2. A comparative calculation reveals less than 5% influence on the quantity of reinforcement.

13. Comparative calculations

As stated above, the main dimensions can change about +/- 10% by calculation according to ENV 1994-2.
Due to serviceability limit states, category C of classification for design criteria has been applied for all comparative calculations. Categories A or B would increase the cost of composite bridges considerably.

14. Advantages and changes of the Eurocodes

Advantages by using ENV 1994-2:

- Economising the amount of steel due to consideration of tension stiffening effect
- Regulation for truss-, bowstring arch- and cable-stayed composite bridges
- Reduction of umbers of shear bolts
- Regulation for different kinds of shear connectors
- Regulations for composite slabs with profiled steel sheeting and composite slabs
- Regulations for decks with precast concrete slabs

Changes by using ENV 1994-2:

- Increase of steel quantity due to fatigue in steel structure
- Increase of reinforcement due to fatigue in concrete slab
- Static analysis becomes more extensive and expensive
- Prestressing tendons are necessary if categories A or B of classification for design criteria are required

15. Conclusion

The ENVs are a compromise of technological usage in different countries and the latest state of research at universities.This endeavour has taken a lot of experts´ time and money. Therefore they should not be applied only for theoretical calculations. All responsible authorities should make the use of the ENVs compulsary for new projects as soon as possible.

Composite bridges are a very economical solution for bridges.
Simple and clear standards are the precondition for a new generation of bridges.

16. References

[1] ENV 1991-3 „Eurocode 1: Basis of design and Actions on structures. Part 3: Traffic loads on bridges“ (1995)
[2] ENV 1992-1 „Eurocode 2: Design of Concrete Structures. Part 1: General rules and rules for buildings“ (1991)
[3] ENV 1992-2 „Eurocode 2: Design of Concrete Structures. Part 2: Concrete Bridges“ (1995)
[4] ENV 1993-1 „Eurocode 3: Design of steel structures. Part 1: General rules and rules for buildings“ (1991)
[5] ENV 1993-2 DRAFT „Eurocode 3: Design of steel structures. Part 2: Steel bridges“ (1996)
[6] ENV 1994-1 „Eurocode 4: Design of composite steel and concrete structures. Part 1: General rules and rules for buildings“ (1992)
[7] ENV 1994-2 DRAFT „Eurocode 4: Design of composite steel and concrete structures. Part 2: Bridges“ (1996)
[8] K. Roik,R Bergmann, J. Haensel, g. Hanswille „Bemessung auf der Grundlage des Eurocode 4 Teil1-1 Sonderdruck aus dem Betonkalender 1993, Ernst & Sohn
[9] F.Tschemmernegg, A. Pattis „Vergleichsstatik Eisenbahnverbundbrücke in Melk“, TU Innsbruck

Composite Bridges for High Performance Lines in Austria Trial calculation according to ENV 1994-2

Johann GLATZL
Dr. tech.
HL-AG
Vienna, Austria

Johann Glatzl, born in 1957, got his civil engineering degree in 1980 and his doctor's degree in 1982 from the Technical University in Vienna. He is head of the bridge construction department at the HL-AG (railway high-performance route Plc.) and lecturer at the technical college for construction engineering in Vienna..

Summary

The application and further development of the composite construction method for railway bridges in Austria is demonstrated by some selected examples. A comparison calculation drawn up for a big railway bridge in Austria shows the differences in the results of the calculations in the comparison of the Austrian standards with the ENV 1994-2

1. Introduction

The political re-organization of Eastern Europe and the completion of the European home market have basically changed Europe at the end of the 20th century. More than ever before Austria - as a country in the heart of Europe - has become a transit country for passenger and freight traffic. A substantial part in mastering the traffic volume has to be taken over by a modern and efficient railway system.

The most important railway lines in Austria will become a part of the trans-European network (TEN). The inclusion in the trans-European railway network requires a certain standard in efficiency, capacity and velocity.

For the planning and the construction of such railway lines the "Eisenbahn-Hochleistungsstrecken-AG" (Railway high-performance route Plc.), or short "HL-AG" was founded in 1989. Our company has focused its activities on the expansion of the east-west-connection between Salzburg and Vienna.

Within the realization of these building projects, the composite method of construction became particularly significant for large bridges.

In the following pages some selected examples for composite bridges in the Austrian railway network will be briefly presented.

2. Railway Bridges in Composite Steel Construction Method

2.1 Gailitzbach Bridge

The Gailitzbach Bridge is situated at the railway line Villach - Tarvis - Pontebba - Udine, which forms one of the main thoroughfares of north-south traffic in the European railway network. Two one-track wing units were established to facilitate the maintenance and the renewal of the wing units. Apart from a reinforced concrete and a prestressed concrete solution a composite steel solution was examined as well. The latter provided for a girder bridge with a central span of 46.5 m, which was haunched in the area of the river crossing and which passed through 6 fields.

2.2 Vienna: A New Access Railway from the Western to the Eastern Railway Line

In the course of this project in Vienna also a draft for a composite bridge for the crossing of the Vienna valley was worked out. A double-tracked composite bridge was planned. The crossing of the road in the Vienna valley was planned with an arched bowstring steel bridge with orthotropic decking and a span of about 100 meters. The spans of the structures in composite steel construction were between 40 and 70 meters.

2.3 New Construction of the Railway Line Vienna - St. Pölten

For the crossing of the valley near Perschling several bridge solutions were worked out. One draft concerned a double-tracked composite bridge with an overall length of 600 meters. The bridge consists of 12 single-span structures with a span of 50 m each. Then main girders were designed as strut-braced trusses.

2.4 St. Pölten Freight Train By-Pass

The crossing of the river Traisen takes place over a three-spanned bridge construction. A draft plans a double-tracked composite steel bridge with solid beam webs, an overall span of about 150 meters and a central span of about 66 meters.

2.5 Railway Bridges over the Melk

In the course of the by-pass of the village of Melk two wing units had to be erected for being able to cross the Melk river and the federal highway B1. An approximately 150-meter-long, two-tracked railway bridge for the high-performance route and an approximately 300-meter-long, two-tracked railway bridge for the access route to the railway station in Melk had to be established. [1]

2.5.1 Bridge drafts - variants

After extensive examination of several variants a haunched -girder bridge with a monocellular box-type cross section was preferred and a composite steel and prestressed concrete version were worked out.

As a result of acoustic examinations the box-type cross section in the composite version was dismissed and an open cross section with two I-beam girders was followed up. According to practical experience and observations composite steel bridges are very suitable for meeting the requirements of modern railway infrastructure in connection with sound radiation because the mass of the wing unit is bigger than in the case of pure steel bridges and the inherent frequency differences of concrete plate and steel structure are so big that coupling effects and regenerative amplification resulting from this can be avoided.

The bridge objects concerned were constructed in such a way that the inherent frequencies of the concrete track plate, of the web plates and the main girder chords show a sufficiently big distance to the critical stimulating frequencies from the railway traffic.

The prevailing experience in railway bridge construction showed that in the case of the present dimensions and span ratios it cannot be said ad hoc whether the cheapest tender result can be reached by a composite steel or rather by a prestressed concrete version. As the tender prices are strongly dependent on the respective market situation, tenders for both composite steel and prestressed concrete versions were invited to reach an optimum economic tender result, and in the comparison of the tenders the maintenance costs were evaluated from the monetary point of view.

This led to the result that the composite steel version, which was more expensive than the prestressed concrete version seen from the tender result, was finally cheaper all in all considering the maintenance and dismantling costs and was therefore further developed.

2.5.2 Description of the structure

The wing unit of the bridge for the high-performance route is a haunched four-field girder with spans of 33 m - 48 m - 33 m and 41 m. The cross section of the wing unit is formed by two haunched web girders of the steel quality S355 JO and thermo-mechanically rolled steel of the quality DIMC-355B with singly reinforced composite plate made of B400 with overhead track. The height of the steel girders varies between 2.60 m at the abutments and 3.90 m at the pillars.

The wing unit of the bridge for the access route to the railway station of Melk is a haunched five-field girder with spans of 53 m - 53 m - 79 m - 53m - 36 m. The cross section of the wing unit is formed by two I-beam girders of the steel quality S355 Jo, thermo-mechanically rolled steel of the quality DIMC-355B and a singly reinforced composite plate made of B500. The height of the structure varies between 3.30 m at the abutments and 5.80 m at the pillars.

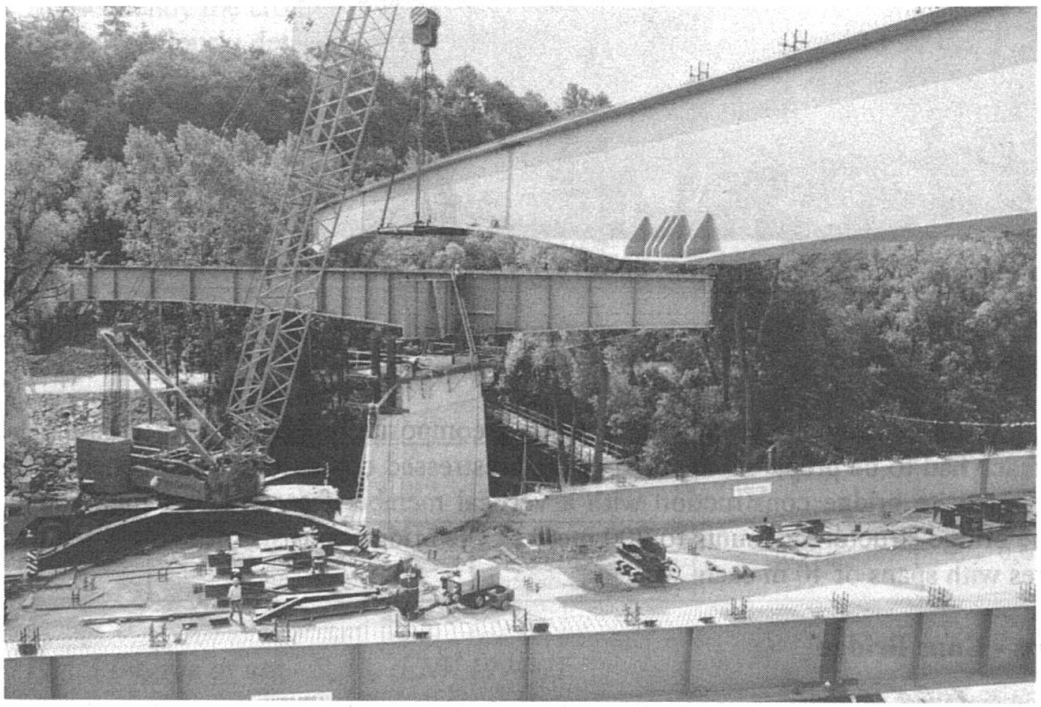

Fig. 1 Hoisting in a span crossing the river

2.5.3 Construction implementation

The approx. 1540-ton-heavy bridge parts were produced from October 1994 to May 1995 in Vienna. The essential parts were established from material with the quality DIMC-355B. Materials up to 90 mm thick were used. The strongest chords consisted of two 90 mm sheets that were up to 1400 mm wide. In the variation of material thickness particular importance was attached to fatigue-resistant construction. In the factory the individual feed scaffoldings with a height of up to 5.20 m, a length of approx. 25 m and a weight of up to 40 tons per piece were welded together. Three feed scaffoldings each, which spanned the river, were welded together to form one unit. The bigger parts with a length of approx. 70 m and weight of approx. 170 tons were mounted by means of mobile cranes. The composite plate of the main bridge was established in the concrete quality B400, that of the access bridge in B500.

The concrete plate is connected to the steel wing unit with setbolts. After completion and age-hardening of the composite plate the wing units were lowered to their final position. During the lowering procedure constructional prestressing of the composite plate was obtained through well-aimed lowering of the pillars.

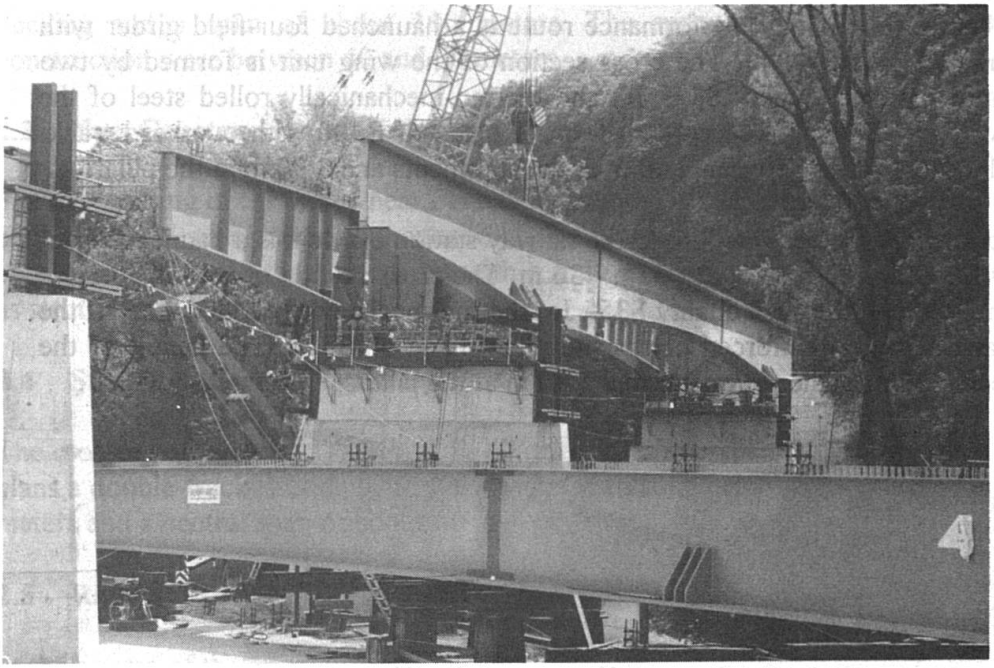

Fig. 2 Establishing and connecting the two main girders of the span crossing the river

2.6 Section Haag - St. Valentin

For the new building of the railway line Haag - St. Valentin a composite bridge draft for crossing the section Haagerbach had to be prepared, apart from the prestressed concrete draft. It concerns a double-tracked composite bridge construction with a vertical member-free strut bracing. The overall length of the bridge structure amounts to 200 meters. The bridge consists of 5 single-span composite structures with spans of 40 m each.

2.7 Enns By-Pass - Enns Bridge

For the bridging of the river Enns two pre-drafts for bridges were worked out, a composite bridge over the main supports and a prestressed concrete bridge solution. The overall span of this bridge project amounts to 413 m; the longest span is 120 m.

2.8 Innsbruck By-Pass

As the last bridge project the Inntal bridge is to be presented. It was erected in the course of the Innsbruck by-pass for which also a composite bridge draft was submitted. The design, however, was carried out as a curved, prestressed, open concrete trough bridge with an overall length of 488 meters. The structures consist of single-span beams with a length of 50 m. This bridge structure is located quite near the town of Innsbruck and spans the river Inn and the Inntal motorway.

3. Consequences of ENV 1994-2 Demonstrated by the Example of the Melk Railway Bridge

For composite steel railway bridges no Austrian standards were available. Therefore a separate calculation basis had to be created for every individual case on the basis of the Austrian norms regulating steel, concrete, composite and railway bridge construction.

In order to be able to study the consequences of the ENV 1994-2 (second draft - 1996), which was in the stage of development a calculation for comparison [4] for the bridge wing unit of the high-performance route in Melk on the basis of ENV 1994-2, was drawn up.

The measurements and material distribution for steel, concrete and reinforcement were taken out from the implementation documents. Then the static analyses for the first compression strut of the bridge construction were carried out according to ENV 1994-2 independently of the implementation statics. The load was calculated according to ENV 1991-3 and then the relevant loading condition combinations for the ultimate limit state (ULS), the serviceability limit state (SLS) and the fatigue limit state (FLS) were determined.

Subsequently the cross section resistance was calculated according to ENV 1994-2 and compared to the previously determined stresses, taking also into consideration the tension stiffening effects above the pillar. The degree of use = S_d/R_d can be seen in the table below for the ultimate limit state (ULS), the serviceability limit state (SLS) and the fatigue limit state (FLS).

	ULS	SLS	FLS
concrete	0,35	1,12	0,58
reinforcement	0,90	0,72	1,29
structure steel top flange	1,12	0,57	0,16(ts) 1,97
studs	0,69	0,67	0,69

Fig. 3 Degree of use - S_d/R_d (ENV 1994-2)

From the table the following can be seen:

- the ultimate limit state (ULS) and the serviceability limit state (SLS) show transgressions of approx. 12% for the structure steel and the concrete, which can be absolutely considered within the range of dispersion of the calculation codes.
- the fatigue limit state (FLS) shows a transgression of approx. 29% in the reinforcement, which leads to an increase of the single reinforcement if determined according to ENV 1994-2 compared to the Austrian norms.
- all three states show that in the case of design of the studs there is a reserve of 30% when calculated according to ENV 1994-2 compared to the Austrian norms, which leads to a significant reduction of the composite means.

All in all it can be ascertained that by calculating according to ENV 1994-2 and by taking into consideration the tension stiffening effects there is an increase in the single reinforcement above the pillar on the one hand and a clear reduction of the composite means on the other.

Thereby the composite action between the concrete track and the main steel girder becomes more elastic, which has a positive effect on the formation of cracks due to the setting heat flowing off and the shrinkage during the setting process of the concrete.

4. Conclusion

As the above statements show today solutions in modern railway bridge construction can be offered with the help of the composite steel construction method, which can optimally meet the requirements from the following points of view:

- efficiency for a modern rail infrastructure
- maintenance and utilization
- preservation of the environment and integration into the landscape
- economic efficiency.

5. References

[1] Glatzl, J.; Pommer, H.: "Neue Eisenbahnbrücken Melk in Stahl-Verbundbauweise" (New Railway Bridges in Melk in Composite Steel Construction Method) Stahlbau-Rundschau (survey on steel construction) 85/1995, p. 24-31

[2] ENV 1991-3 "Eurocode 1: Basis of design actions on structures. Part 3: Traffic loads on bridges" (1994)

[3] ENV 1994-2 (Second draft) "Eurocode 4: Design of composite steel and concrete structures. Part 2: Bridges" (1996)

[4] Tschemmernegg, F., Pattis, A.: "Vergleichsstatistik Eisenbahnbrücken Melk" (Comparison of Statics of the Railway Bridges in Melk), TU (Technical University) in Innsbruck

A Comparison of Standard Test Methods for Flexural Toughness of FRC

Petia STANEVA
Senior Researcher
Regional Science Inst.
Sapporo, Japan

Takashi HORIGUCHI
Professor
Hokkaido Inst. of Techn.
Sapporo, Japan

Koji SAKAI
Head of Material Section
Civil Eng. Research Institute
Sapporo, Japan

Summary

The significance of energy absorption of the fiber reinforced concrete (FRC) for its performance in the structures motivates the attempts to determine the most proper test procedure for FRC toughness characterization. This paper presents the results of study on determination of correlation among various standards and recommended test methods for flexural behavior and primarily for flexural toughness of FRC . Compressive toughness behavior is of concern as well.

1. Introduction

The basic difference between the plain concrete and fiber reinforced concrete is found in their toughness performance. The significance of energy absorption capability for the materials and structural design motivates the further developments of various test procedures for better description of toughness performance. The toughness is considered as a compressive, tensile, flexural etc. toughness. Usually, the flexural toughness is determined according to ASTM requirements [1], JCI recommendations [2] and ACI recommendations [3]. The most recent studies proved that the obligatory determined I_5, I_{10} and $R_{5,10}$ are not sensitive to the fiber type and volume, and that is more valid for small size of test specimens (like 100x100x150 or 150x150x450 mm) [4]. The higher indices I_{20}, I_{30} etc. and JCI parameters are pointed out to be more descriptive for the improvement in flexural toughness due to fiber volume or type. Another test method describes very well the post-peak part of the load-deflection curve and therefore the toughness performance [5].

The importance of first crack deflection was shown and a new, more practical proposal for a determination of a flexural parameter was given in order to estimate first crack deflection influence on the toughness parameters. Very comprehensive research is done on the effect of seating and twisting of supports on the mid-span deflection [6,7] and most of the experiments considered that problem by using a special frame as described in [2,7,8,10]. The specimen geometry and size influence the toughness expressed through ASTM indices, which was reported in recent studies unless the specimens are in geometrical similarity [4]. In some of the analyses [4], it was stressed that more attention should be paid to residual strength factor like $R_{30,50}$ or $R_{80,100}$ which are more meaningful for the design because they would express the average load over a portion of load-deflection curve preceding the specified end-point deflection.

The properties of plain concrete are well studied in cases involving different temperatures, especially subzero ones [9] and thermal shock. In last decade, the studies on FRC behavior at low temperatures aimed to fill the gap in the knowledge for toughness behavior at low temperatures.

The objective of this study is to find and analyze how the different standard test methods and parameters describe the toughness behavior of FRC tested not only at normal (20deg) temperature as required in the specifications, but at low temperatures like -20 or -50 deg. The correlation among the toughness parameters of different test methods would explain to what degree those methods are applicable to different than specified test conditions.

2. Experimental Program and Reference Experiment Details

2.1 Details of Authors` Experiment

In the experiment conducted, the flexural toughness behavior was studied in terms of different fiber type, fiber volume and testing temperature. Steel fibers were applied in two types differed by shape and in 5 volumes (0.5; 1.0; 1.5; 2.0; 2.5%). Three test temperatures were chosen - +20; -20; -50 deg. The testing machine was a hydraulic type with a load control. The loading speed maintained a constant increase in the stress. The size of test specimens was 100x100x420 mm with a mid-span of 300mm. The load-deflection curves were measured and toughness parameters were determined according to ASTM (I_i and $R_{i,i+1}$) and JCI. More details on the experimental program are given in [10,11].

2.2 Details of Reference Experiments

2.2.1. Experiment by Horiguchi etc. [12]
The main objective of this experimental program was to study the compressive, pull-out and flexural toughness behavior of hybrid fiber reinforced concrete (HFRC) at different temperatures. Two fiber materials were applied: steel and vinylon. Steel fibers (S) were presented in 4 types which differed mainly in length, shape and aspect ratio. Vinylon fibers (V) were two types with different lengths. HFRC mixes with total 1% (.5S+.5V); 1.5% (.5S+1.0V); 1.5% (1.0S+.5V) fiber inclusion were produced. Compressive and flexural test were conducted both at +20; -20 deg. The loading machine in compression was with a load control and that in flexure - with a deflection control. The test specimens for flexural test were beams 100x100x400 mm in size and with a mid-span of 300 mm, and those for compressive test were cylinders 200x100 mm in size. The load-deflection curves in compression were measured and the toughness parameter according to JCI was calculated. The load-deflection curves in flexure were also recorded and based on the procedure described in ASTM [1] and ACI [3] both I_{30} and I_{075} were calculated respectively. Also the parameter FF, proposed in [5] and which should be independent of fiber amount for fiber types assuring good toughness, was determined.
2.2.2. Experiment by Banthia etc. [13]
The main purpose of this experimental program was to extend the limited data for FRC behavior at low temperatures. Here again two fiber materials were applied: steel and carbon. Steel fibers were described as macro (SMa) and micro (SMi) fibers, and carbon fibers (C) were only micro one. Fiber volumes used were 1%SMa; 2% (1.0SMa+1.0SMi); 2% (1.0SMa+1.0C). Testing temperatures were set at 22 and -50 deg. A deflection control type

loading machine was used. The flexural test specimens were beams 50x50x450 mm in size with a mid-span of 300 mm. The load-deflection curves were recorded and the flexural toughness according to JCI [2] was provided and I_{30} indices calculated. All details mentioned above are summarized in Table 1.

References	Fiber Material	Fiber Type	Type of Concrete	Fiber Volumes, %	Specimen' Size, mm	Loading Type	Temperature Range, deg
Authors [10,11]	Steel	2	SFRC	5(0.5;1;1.5; 2;2.5)	100/100/300	Load control	20; -20; -50
[12]	Steel; Vinylon	6	HFRC VFRC	2 (1; 1.5)	100/100/300	Deflection control	20; -20
[13]	Steel; Carbon	3	SFRC CFRC	2(1; 2)	50/50/450	Deflection control	20; -50
Compressive Test							
[12]	Steel; Vinylon	6	HFRC	2 (1; 1.5)	100/200	Load control	20; -20

Table 1 Details of the experiments in consideration

3. Results and Discussion

3.1 Compressive Toughness Parameters

The compressive test results of [12] are considered through JCI recommendations [2] for a compressive toughness , which is the area under load-deflection curve up to 0.75% of the deflection measured. Also, an average compressive strength was calculated at 0.75% change of the specimen height. Both were determined at normal and low (-20 deg) temperatures. The plotted results and a function of compressive strength and toughness correlation are shown in Fig. 1. The compressive strength at 20 deg and at -20 deg are in a linear relationship and an increase in the strength at 20 deg is maintained as an increase in the strength at -20 deg as well. The compressive toughness at both temperatures does not show high correlation. While the toughness at normal temperature increase with the fiber inclusion, the toughness at low temperature did not change significantly and kept almost the constant value. The hybrid fiber inclusion benefits the toughness at normal conditions, but concrete matrix behavior at low temperature still influenced strongly the hybrid FRC compressive toughness at those conditions.

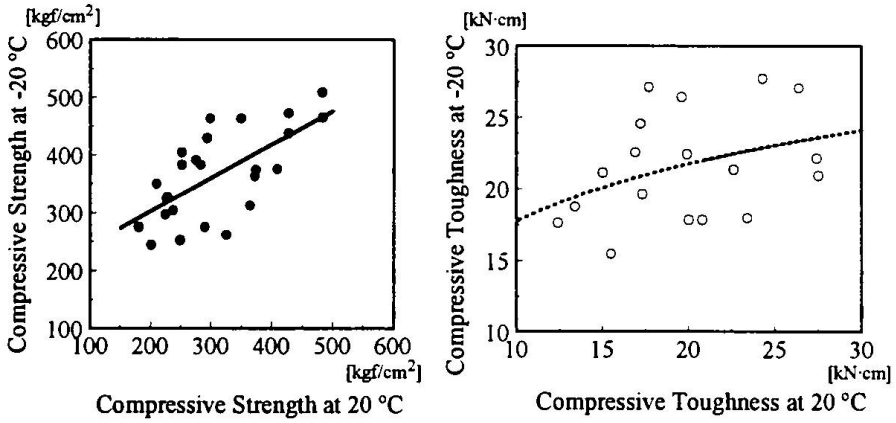

Fig.1 Compressive strength and toughness at 20 and -20 deg

Knowing the compressive strength at normal conditions, it is likely to predict it at low temperature, which is not valid for the compressive toughness because of the low correlation found. No correlation was found between ASTM I_{30} and compressive toughness at all temperatures either.

3.2 Flexural Toughness Parameters

The results reported in [10,11] and their analysis showed that the toughness increased while fiber volume increased at all temperatures tested. Also that was indicated by all test methods - JCI, ASTM. A some contradictions appeared when comparing the overall performance in flexural toughness of SFRC at all temperatures. The toughness factor T according to JCI, showed an improvement in the performance while temperature was changed from 20 deg to -50 deg. On the other hand, ASTM I_{20}, I_{30}, I_{50} and I_{100} indices showed a decrease in the performance at the same conditions. The I_i lines presented in Fig. 2 show that I_5 and I_{10} could not be used for a precise description of the toughness at -20, -50 deg. A better description can be achieved by using higher indices I_{30} and more, at -20, -50 deg. The difference in the flexural performance expressed through I_{20}, I_{30}, I_{50} and I_{100} is more obvious when comparing 20 and -20 deg and very slight between -20 and -50 deg. When plotted, the results of [13] which are for different type fibers fitted well with the I_{30} results of [10,11].

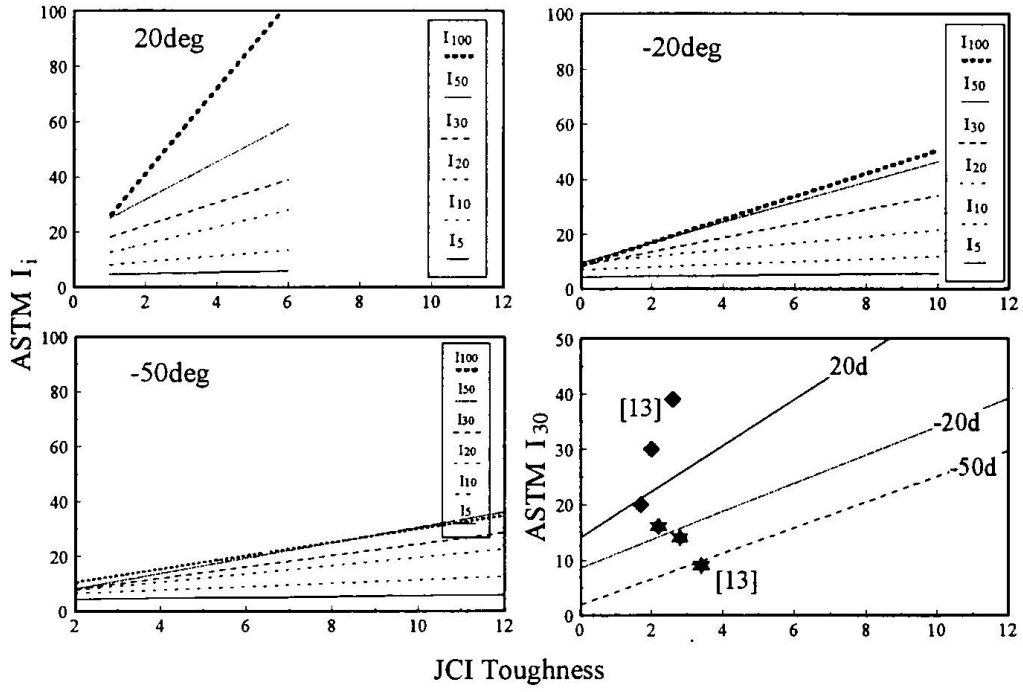

Fig.2 Toughness correlation of T and I_i at different temperatures

The analysis of results of [12] is shown as a I_{075}-I_{30} relationship. It was reported previously that a linear relationship was found at low temperature, and a quadratic relationship at normal temperature. Therefore, the both procedures [1,3] equally describe the flexural toughness at low temperature, but I_{30} is a better measure at normal temperature, as shown in Fig. 3. On the other hand, it was not found any pronounced correlation between I_{30} and FF, where FF is a parameter which describes the post-peak part of load-deflection curve at a deflection with crack width of 1mm, at both temperatures considered. The possible

explanation for this result is the small test specimen size used. Further study on different sizes and at low temperature is necessary for an identifying FF parameter usefulness.

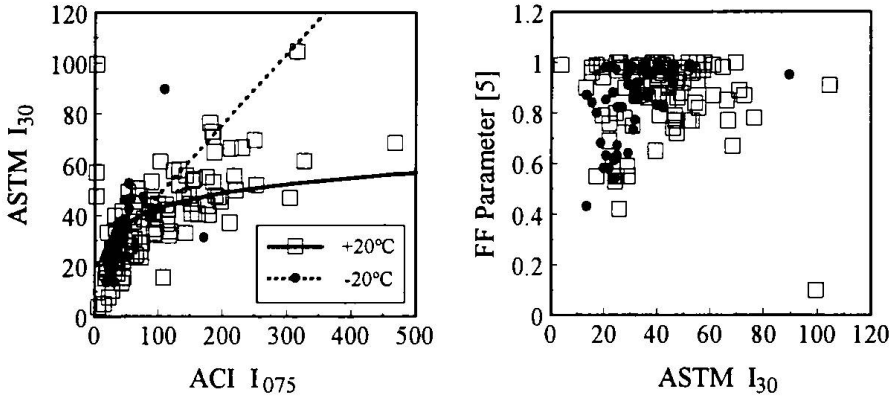

Fig.3 Toughness indices I_{075} - I_{30}, and I_{30} - FF relationships

Next, the toughness factor [2] and residual factors $R_{5,10}$, $R_{10,20}$, $R_{20,30}$ and $R_{30,50}$ relationships are shown in Fig.4. With the decrease of the temperature, residual strengths decrease and the area between $R_{5,10}$ and $R_{30,50}$ increases with the decrease of the temperature. Then the residual strength factor becomes more sensitive to low temperature and therefore good way for a description of flexural toughness performance of FRC.

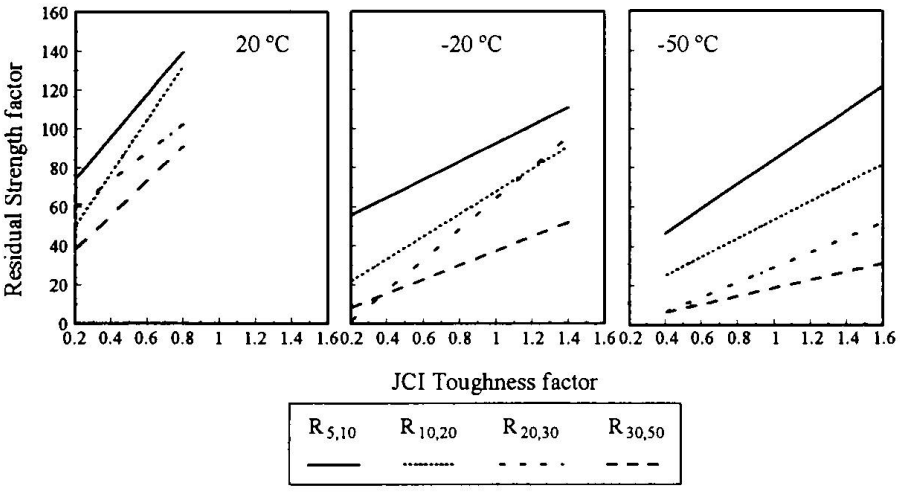

Fig.4 Residual strength factors at different temperatures

4. Conclusion

Next conclusions can be drawn based on the results and their analysis.

- The compressive strength at low temperature does not show an improvement and no correlation is found between the compressive toughness at both temperatures.
- It is confirmed that I_5, I_{10} and $R_{5,10}$ are not sensitive for a distinction of flexural

toughness at different temperatures, but using the indices I_{30} and higher, residual strength factors $R_{20,30}$ and higher would be a better way for flexural toughness characterization.

- ACI I_{075} index could be used for describing flexural toughness performance in the same order as ASTM I_{30} at low temperatures.

- The toughness factor T according to JCI is not very appropriate measure when considering low temperatures.

References

1. Standard Test Method for Flexural Toughness and First-Crack Strength of Fiber Reinforced Concrete". ASTM Standards for Concrete and Mineral Aggregates, V.04.02, Standard Designation C1018, 1991, pp. 7.
2. "JCI Standards for Test Methods of Fiber Reinforced Concrete". Japan Concrete Institute, February 1984, pp. 45-51.
3. ACI Committee 544. "State-of-Art Report on Fiber Reinforced Concrete". ACI Manual on Concrete Practice, Part 5, American Concrete Institute, Detroit, 1991, pp. 22.
4. Chen, L., Mindess, S., Morgan, D. R., et al. " Comparative Toughness Testing of Fiber Reinforced Concrete". Testing of Fiber Reinforced Concrete, ACI SP-155, American Concrete Institute, Detroit, 1995, pp. 41-75 .
5. Lorentsen, M. " Steel Fiber Concrete for Structural Elements". Proceeding of US-Sweden Joint Seminar "Steel Fiber Concrete", Stockholm, 1985, pp. 421- 442.
6. Gopalaratnam, V. S., Shah, S. P., Batson, G. B. et al. "Fracture Toughness of Fiber Reinforced Concrete". ACI Materials Journal, Vol. 88, No 4, July-August 1991, pp. 339-353.
7. Balaguru, P., Narahari, R. and Patel, M. " Flexural Toughness of Steel Fiber Reinforced Concrete". ACI Materials Journal, Vol. 89, No6, November - December 1992, pp. 541-546.
8. Banthia, N. and Mani, M. " Toughness Indices of Steel Fiber Reinforced Concrete at Low Temperatures". Second Canada-Japan Workshop on "Low Temperature Effects on Concrete", Proceedings, 1991, pp. 269-279.
9. Rostacy, F.S., Schneider, U. and Wiedeman, G. " Behavior of Mortar and Concrete at Extremely Low Temperatures".Cement and Concrete Research, Vol. 9, No3, 1979, pp. 365 - 376.
10. Staneva, P., Sakai, K., Horiguchi, T. et al. " Flexural Behavior of Steel Fiber Reinforced Concrete under Low Temperatures". Proceedings, 15 th Annual Convention of Japan Concrete Institute, Kobe, Japan, Vol. 1, June, 1993.
11. Staneva, P., Sakai, K., Horiguchi, T. et al. "Flexural Strength and Flexural Toughness Indices of Steel Fiber Reinforced Concrete under Low Temperatures". 7th International Conference of Composite Materials, Sofia, Bulgaria, 1994.
12. Horiguchi, T., Takamichi, H. and Sakai, K. " Flexural and Compressive Toughness of Hybrid Fiber Reinforced Concrete". Proceedings of Symposium on Application of Advanced Reinforcing Materials to Concrete Structures, Sapporo, November, 1996, pp. 117-124. (in Japanese)
13. Banthia, N., Qu., L. and Sakai, K. " Strength and Toughness of Fiber Reinforced Concrete at Low Temperatures". Concrete Under Severe Conditions, E&FN Spon, Vol. 2, pp. 1428-1437.